64-5

AIR FORCE INSTITUTE OF TECHNOLOGY

AIR UNIVERSITY
UNITED STATES AIR FORCE

SCHOOL OF ENGINEERING

WRIGHT-PATTERSON AIR FORCE BASE, OHIO

AF-WP-O-OCT 63 2,500

DETERMINATION OF ELECTRON ENERGY DISTRIBUTION IN AN ARGON RF PLASMA

Lt Raymond T. Bourket, Jr.

GNE/Phys/63-3

DETERMINATION OF ELECTRON ENERGY DISTRIBUTION IN AN ARGON RF PLASMA

THESIS

Presented to the Faculty of the School of Engineering of
the Air Force Institute of Technology
Air University
in Partial Fulfillment of the
Requirements for the Degree of
Master of Science

By
Raymond Thomas Beurket, Jr., B.S.
Lieutenant USA
Graduate Nuclear Engineering

August 1963

Preface

This report was undertaken mainly for the purpose of determining the electron energy distribution in an argon RF excited plasma since up until the writing of this report, no energy distribution measurements have been made in any RF plasma. I have written this report with the hope that a person with a general physics background but with little or no knowledge of plasmas can appreciate how energy distributions of electrons in plasmas may be determined and specifically how they may be made in RF excited plasmas.

Perhaps the most valuable aspect of this investigation (in addition to accomplishing what I set out to do) was the discovery that no matter how simple a problem sounds on paper, unexpected difficulties always seem to crop up when new ideas are tried. Therefore, in scheduling a project I have found that time must be set aside to iron out any unforeseen difficulties that might arise.

In conducting this investigation I received valuable assistance from the members of the Electronic Technology Laboratory at Wright-Patterson Air Force Base. I am indebted to Mr. David L. Mays for his most painstaking explanation of equipment and helpful suggestions and to Mr. E. Mason Friar for the use of his radio transmitter. I am also indebted to Mr. Werner F. Jehn for the construction of the spherical probe, for his help with the vacuum system, and for his humor which kept up the author's morale.

I wish to express my appreciation to Dr. Gustav K. Medicus for his explanation of the more complex aspects of probe theory and for all the suggestions he made throughout the experiment. I also wish to express my appreciation to Professor La Verne Lewis who was my thesis adviser, and to Dr. William C. Eppers who sponsored the project and made the equipment available to me.

Raymond T. Beurket, Jr.

Contents

Contents

List of Figures

List of Tables

Abstract

This investigation determined that electron energy distribution measurements in an RF excited plasma are feasible if the plasma is excited by a cylindrical coil fed push-pull from a balanced power source and if probe measurements are made along the axis of the coil. As far as is known, the measurements made during this investigation are the first energy measurements made in an RF plasma.

The basic theory of plasma generation and general probe theory were reviewed; Medicus' spherical probe theory was used in making the determinations. Experimental equipment was designed and built and suggestions for improvement were made.

The results indicated that in the argon RF plasma of this investigation, the energy distribution is markedly non-Maxwellian.

GNE/Phys/63-3

DETERMINATION OF ELECTRON ENERGY DISTRIBUTION IN AN ARGON RF PLASMA

I. Introduction

Forty years ago Langmuir gave the name plasma to partly ionized gas in which the positive and negative charges are approximately equal and developed the basic plasma theory (Ref 8:3). Since Langmuir's time, the field of plasma physics has been expanded greatly. Plasma theory is not only an interesting subject but is important since probably 99.9% of matter in our universe is in the plasma state (Ref 8:2). Thus, the study of plasma is indeed worthwhile.

This report deals with one area of plasma physics, the determination of electron energy distribution in an RF excited plasma. It is important because the results of this experiment may shed light in other areas of investigation. The Electronic Technology Laboratory at Wright-Patterson is currently doing studies on the gaseous laser. As an extension of this thesis topic it may be possible to determine the electron energy distribution in the laser with the hope of using the information obtained to try to optimize the laser's efficiency.

At present no work has been done in making energy measurements in an RF plasma, and the main objective of this report was to determine if meaningful measurements could be made. Measurements were made in a cylindrical argon filled tube with the restriction that the measurements

were made only along the center line of the tube. The reason for this restriction will be made apparent in Chapter II.

This report is divided into five main parts:

(1) A discussion of the formation and properties of a plasma, including an analysis of the conditions under which measurements can be made in an RF plasma;

(2) A discussion of probe theory in general;

(3) A discussion of spherical probe theory;

(4) A discussion of the equipment used in the experiment;

(5) Results and conclusions.

A computer program which was used in reducing the data may be found in Appendix A. Semi-log plots of the second derivative of the probe curves may be found in Appendix B.

II. Plasma Characteristics

Formation and Properties of a Plasma

When an electric field is applied to a gas at atmospheric pressure, the gas will act as a good dielectric unless the electric field is extremely strong. If the pressure of the gas is reduced sufficiently and the field is held constant, the gas will become conducting and the gas may glow with a color characteristic of the gas employed (Ref 1:132). In this experiment argon gas was used and the resulting plasma was pink.

The field applied to the gas may be either a DC or RF field. The DC field may be generated if a potential is applied between two electrodes placed in the gas. The RF field may be produced by surrounding the gas with a coil and then applying RF energy to the coil.

Ionization by Electrons. The conducting properties of the gas and the glow are caused by partial ionization of the gas and subsequent recombination. This partial ionization of the gas is caused by the acceleration of electrons by the electric field and their resultant energy loss by inelastic collision with gas atoms. The primary exciting electrons may occur initially as a result of the interaction of cosmic rays with the gas (Ref 14:27). If this naturally occurring process is not sufficient to produce the necessary initial source of electrons for the creation of the plasma, an external source of electrons may be provided (as was the case in this experiment) by placing a Tesla coil near the tube containing the gas. Once these primary electrons have been provided and the pressure of the gas and applied electric field strength

have been properly adjusted, the plasma should become self-sustaining since each ionisation will produce at least one additional electron capable of causing further ionisations until a balance between generation of electrons and loss of electrons is achieved.

It is well known that a particle of charge q when falling through a potential V will achieve a kinetic energy qV. In order to more fully understand the method by which ionisation takes place, it is necessary to understand how the electrons lose their kinetic energy. Upon achieving a certain kinetic energy, the electrons will proceed to lose their energy in four principal ways (Ref 14:16):

(1) The electrons surrender energy upon suffering collisions at the wall of the tube and to the anode in a DC discharge.

(2) The electrons transfer energy to the gas in the form of heat as a result of elastic collisions.

(3) The electrons excite the gas atoms as a result of inelastic collisions.

(4) The electrons ionize the gas atoms after colliding inelastically.

In addition, in an RF plasma, those electrons whose direction of motion is against the electric field will also lose kinetic energy.

Since gas atoms of atomic weight A have 1840 A the mass of an electron (an argon atom has 73,600 times the mass of an electron), the energy loss by the electrons upon elastic collision with gas atoms will be so small as to be negligible. This can be shown to be true if the equations of conservation of energy and momentum are considered and the

electron and atom are assumed to be small elastic spheres. Thus even though the electrons suffer elastic collisions in falling through a potential V their kinetic energies will still be qV to a high degree of accuracy (Ref 14:11).

If the energy of the electrons is greater than the energy equivalent of the ionization potential of the gas, the electrons may ionize the gas upon colliding inelastically with a gas atom. If the energy of the electron is less than the energy equivalent of the ionization potential, the electron will lose energy upon an inelastic collision with a gas atom and will excite the atom. As long as the energy gained by the electron is less than the lowest excitation level of the gas atom, all collisions must be elastic and if all the electrons have energies that low, no plasma can exist.

The electric field strength and pressure must be correct to insure a plasma because the potential through which the electrons fall per collision is the factor that determines whether they will achieve enough energy to cause excitation or ionization. The average distance between collisions is known as the mean free path of an electron in the gas, and its symbol is λ. If the electric field strength is symbolized by E, then the potential difference per mean free path is $E\lambda$. Since λ represents the average distance between collisions, if the number of particles increases, then λ must decrease. This is equivalent to saying that as the pressure rises, the mean free path drops. Thus, there is an inverse relation between mean free path, λ, and pressure p; hence,

the potential difference per mean free path will be proportional to E/p (Ref 14:16). In order to achieve excitation or ionization, the ratio E/p must be adjusted so that it is large enough to insure that the potential per mean free path is large enough that the electron will gain enough energy after several mean free paths to excite or ionize the atom. This may be accomplished by increasing the field strength or lowering the pressure. In this experiment, the pressure was set at 0.2 torr which was sufficiently low for the field intensity involved to give a dense plasma.

Ionization by Ions and Photons. At this point, mention will be made of the positive ions and their roles in causing ionization. Positive ions are formed whenever an electron is ejected from a neutral atom. These ions will also gain kinetic energy as a result of being accelerated by the electric field. The masses of the ions are essentially the same as the masses of the neutral gas atom since the loss of an electron will affect their masses negligibly. Since the ions have about the same mass as the neutral gas atoms, the ions will lose most of their energy after each collision and hence in most cases never gain enough energy to excite or ionize the gas atoms. Thus, we can essentially ignore the effect of excitation or ionization caused by ions (Ref 14:18).

Electrons may also be liberated by the photoelectric effect, but this contribution is very minor too. The wavelength of the photons must be short enough to cause excitation or ionization and this is rarely the case. The principal means of ionization, therefore, is by the inelastic collision of electrons with gas atoms.

Conditions Necessary for Probe Measurements

Since the number of positively and negatively charged particles in the plasma is essentially the same, the net space charge in the plasma region is zero. In a DC plasma the potential drop of the tube occurs across the cathode and the positive ion sheath that forms very near it. The rest of the plasma is essentially field free. This is fortunate because when a plasma is probed, the probe must be in a field-free region in order to make meaningful measurements. In the RF case, the electric field will penetrate the plasma and the field lines will be concentric about the axis. Probe measurements are not impossible in the RF plasma if the probe is restricted to the axis of the tube and a push-pull feed is used to excite the plasma. With this arrangement there will be no RF potential between probe and plasma and the probe will lie in a field-free region as the following discussion indicates.

If the plasma is generated by feeding push-pull a coil surrounding the plasma tube, two important conditions occur in the tube. First, a ground plane will exist in the tube if the electrical center of the coil is grounded. Secondly, at the geometrical center of the tube the RF electric field should be zero if the exciting frequency is not too high.

Ground Plane. Feeding the coil push-pull implies that the voltage impressed on one side of the coil will be 180° out of phase with the voltage impressed on the other side. If the voltages are balanced and if X (Fig. 1, shown on the following page), the electrical center of

the coil, is grounded, a ground plane XA is expected in the tube as a result of the symmetry of the coil and the push-pull feed.

Field-Free Region. If the exciting frequency is not too high, i.e., if its associated wavelength is long compared to the circumference of the coil, then the current at any point of the coil at any instant of time is constant and thus the current I(t) is independent of position. The magnetic field at position r may be found by use of Ampere's Law,

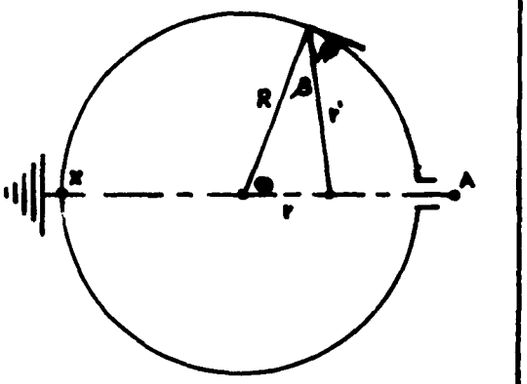

Fig. 1
Top View of Exciting Coil

$$B = \frac{\mu I(t)}{4\pi} \int_0^{2\pi} \frac{R \sin\theta \, d\theta}{r'^2} \tag{1}$$

But by using the law of cosines in Fig. 1

$$r'^2 = r^2 + R^2 - 2rR\cos\theta \tag{2}$$

and

$$\cos\beta = \frac{R^2 + r'^2 - r^2}{2Rr'} = \sin\varphi \tag{3}$$

Substituting Eq (2) into Eq (3)

$$\sin\varphi = \frac{R^2 + r^2 + R^2 - 2rR\cos\theta - r^2}{2Rr'} \tag{4}$$

Substituting Eqs (2) and (4) into Eq (1) and simplifying

$$B_{(r)} = \frac{\mu I(t)}{4\pi} \int_0^{2\pi} \frac{(R^2 - rR\cos\theta)d\theta}{\left[R^2 + r^2 - 2rR\cos\theta\right]^{3/2}} \tag{5}$$

Equation (5) is not integrable in closed form.

By assuming that the wavelength associated with the exciting frequency was long with respect to the coil dimension, Eq (5) was derived in which B is a function of r and t only. Thus the magnetic flux lines are symmetric about the axis and consequently the lines of force representing the electric field E will form closed concentric loops about the axis.

Faraday's Law states that

$$\oint \mathbf{E} \cdot d\mathbf{l} = -\int \frac{\partial \mathbf{B}}{\partial t} \cdot d\mathbf{A} \tag{6}$$

Although Eq (5) cannot be integrated in closed form, $B_{(r)}$ may be evaluated at $r = 0$, which is a point of considerable interest, yielding

$$B_{(0)} = \frac{\mu I(t)}{2R} \tag{7}$$

Since $B(r,t)$ is finite at $r = 0$ and is a continuous function everywhere inside the coil, it will be assumed that in the interval from $r = 0$ to $r = \Delta r$ that $B_{(r)}$ is constant at any time t and is given by Eq (7). Solving Eq (6) for E yields

$$\int_0^{2\pi} E \cdot r d\theta = \frac{-\mu}{2R} \frac{\partial I(t)}{\partial t} \int_0^{\Delta r} \int_0^{2\pi} r dr d\theta \tag{8}$$

$$E \cdot 2\pi r = \frac{-\mu}{2R} \frac{\partial I(t)}{\partial t} \pi r^2 \Big]_0^{\Delta r} \tag{9}$$

$$E = \frac{-\mu}{4R} \frac{\partial I(t)}{\partial t} \Delta r \tag{10}$$

Therefore,

$$\lim_{\Delta r \to 0} E = 0 \tag{11}$$

From the preceding discussion, it is seen that the probe must be positioned along the axis of the tube to avoid RF pick-up by the probe and to prevent the electrons from being accelerated to the probe by the electric field.

III. General Probe Theory

Langmuir was the first to do an adequate study of the theory of electron collection by probes. Later he and Mott-Smith published a paper in October, 1926 (Ref 13) which is a valuable reference for probe theory. Druyvesteyn, however, was the first to show that the second derivative of probe current with respect to probe voltage in the electron retarding region is proportional to the energy distribution of the electrons in the plasma. In 1961 Medicus developed the theory of spherical probes (Ref 11) using an impact parameter approach to the problem. His theory has the advantage over Druyvesteyn's in that although it yields the same results, it is much simpler to comprehend. To apply Medicus' theory in its entirety the data, however, obtained from probing a plasma must come from a small spherical probe.

The electrons in the plasma may assume any type of distribution in Medicus' theory, and his theory will apply to RF excited plasmas as well as DC excited plasmas, providing there is no RF potential between the probe and the plasma and the probe is in a field-free region. In both the DC and RF cases, the probe must be small (diameter on the order of 0.5 mm) to insure that the probe does not distort the plasma appreciably. Since Medicus' analysis of electron energy distributions depends on data from probes, an understanding of the current collecting mechanism of probes is important.

The Probe Negative with Respect to Plasma Potential

When a probe is placed in a plasma at a potential strongly negative with respect to the plasma, the probe will repel electrons and attract ions. A positive ion sheath will build up around the probe. Beyond the positive ion sheath there exists a pre-sheath which contains both positive and negative carriers and beyond this pre-sheath lies the undisturbed plasma. The probe current at the strongly negative potential will consist entirely of an ion current as region A, Fig. 2 indicates.

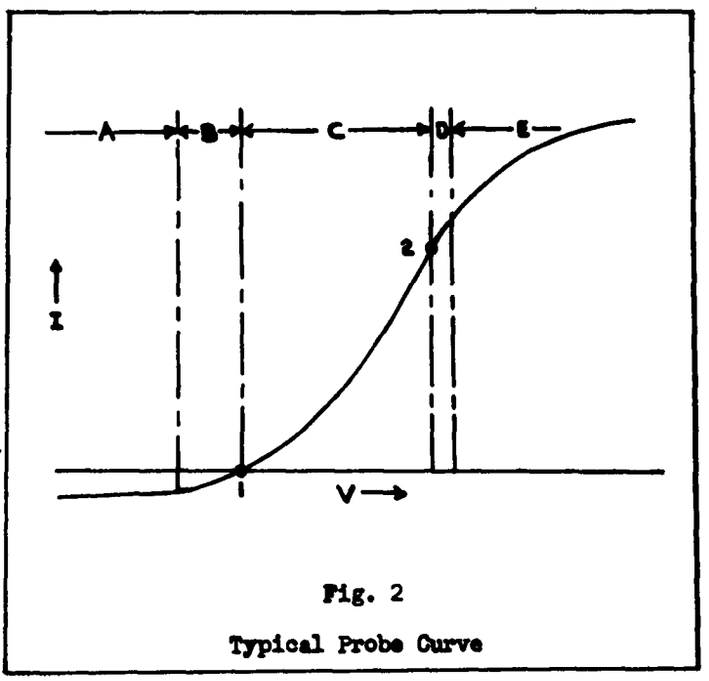

Fig. 2
Typical Probe Curve

As the potential of the probe is made more positive with respect to the plasma (although it still remains negative with respect to the plasma) some of the higher energy electrons will overcome the probe-to-plasma retarding potential and will strike the probe and be collected. In addition positive ions will still be accelerated to the probe so the resulting current will be the ion current minus the

electron current. Thus the current collected by the probe falls off as region B, Fig. 2 indicates. The sheath around the probe will no longer be a pure positive ion sheath since electrons can penetrate it, but will have the characteristics of a pre-sheath. As the probe is made even more positive with respect to the plasma a point will be reached, point 1, Fig. 2, in which the rate of collection of ions and electrons is the same. Therefore, the probe will draw zero current. This is the potential at which an insulated probe will stabilize when placed in a plasma and therefore is called floating potential. As was mentioned in Chapter II, an ion will never achieve the energy of an electron because of the comparability of ion and neutral gas atom mass; hence, the insulated probe will stabilize at a negative potential because the electron velocity on the average must be greater than the positive ion velocity. Thus, more electrons will diffuse to the probe per unit time than positive ions. Since the probe is insulated, no current can flow. The potential of the probe will then build up to that negative value at which sufficient numbers of the electrons are repelled to cause the electron and ion collection rates to be the same. Theoretically, the use of the insulated probe was one of the earliest methods for determining plasma potential as it was erroneously assumed that an insulated probe would assume the potential of the plasma (Ref 12:315).

When the probe is made more positive than floating potential, more of the electrons in the high range of the electron energy spectrum will overcome the probe-to-plasma retarding potential and will

be collected. The probe current will then be equal to the electron current minus the positive ion current and thus will appear as an electron current as region C, Fig. 2, indicates.

The Probe at Plasma Potential and Higher

Finally, if the probe is made even more positive, it will reach a potential equal to plasma potential, point 2, Fig. 2, and theoretically electrons and ions of all energies will reach the probe. For the probe curve of Fig. 2, plasma potential is reached at the point where the probe curve inflects as will be shown in Chapter IV. In the region ranging from the probe at the potential at which the highest energy electron may be collected to the probe at slightly less than plasma potential, i.e., regions B and C, the sheath around the probe contains both positive and negative carriers. This region is generally known as the electron-retarding region. At plasma potential there is no sheath around the probe because the probe neither attracts nor repels electrons or ions. Thus, the electrons and ions that reach the probe reach the probe by diffusion only.

Making the probe more positive than plasma potential will cause electrons to be accelerated and the positive ions to be repelled as region D, Fig. 2, indicates. The sheath around the probe will be an electron sheath containing predominantly electrons but also those ions with energies high enough to overcome the probe-to-plasma potential. Increasing the potential of the probe sufficiently, region E, Fig. 2, causes all ions to be repelled and also causes an exclusively electron

sheath to form around the probe. A curve such as that in Fig. 2 may be automatically plotted as will be discussed in Chapter V.

Region of Interest for Energy Distribution Measurements

The primary region of interest for determining energy distributions is the electron retarding region. As has been shown, the magnitude of the probe current varies as the probe-to-plasma potential is varied. This change in the electron retarding region, as already discussed, is a result of the fact that electrons with lower energies are able to overcome the probe-to-plasma potential as the potential is made more positive, until finally at plasma potential electrons of all energies will be collected. Intuitively then there should be a relationship between the electron energy distribution of the plasma, the probe current and the probe potential. The next chapter will show how they are related.

IV. Spherical Probe Theory

Medicus' spherical probe theory, which he proposed in the Journal of Applied Physics in December, 1961, was used exclusively in this project and will be discussed in this chapter. This chapter parallels his spherical probe theory (Ref 11) in showing the relationship between the energy distribution of the electrons in the plasma, the probe current and the probe potential, but this author has found it more advantageous to this paper to derive all equations in terms of energy distribution functions rather than velocity distribution functions as was done by Medicus. The equation used by Medicus for determining current density will be derived by this author on the basis of electron scattering. The location of plasma potential on the probe curve will be shown as a logical extension of Medicus' spherical probe theory.

Mott-Smith and Langmuir in 1926 devised equations for electron collection in an article in Physical Review but suggested an alternate attack which consisted of subdividing the flow of electrons into parallel moving swarms of electrons (Ref 13:751). Medicus has used this approach in developing his theory of electron collection by the spherical probe.

Probe Collection of an Isotropic Distribution of Monoenergetic Electrons

If a probe having a radius r_p is immersed in a hypothetical plasma containing monoenergetic electrons and is at the potential of the plasma in an actual case it will collect ions and electrons which

diffuse to the probe. The fact that ions diffuse to the probe when it is at plasma potential and are attracted to the probe when it is negative with respect to the plasma will be ignored in the following derivations as the effect of the positive ion current will later be quantitatively shown to be small. For the purpose of this derivation then the positive ions will be assumed to be in the plasma for the sole purpose of preserving space charge neutrality and will not be collected by the probe.

The current collected by the probe will therefore be purely an electron current and will be equal to the product of the collecting area of the probe and the electron current density. If it is assumed that the distributions of the electrons in the hypothetical plasma are isotropic and each electron has the same speed v then the electron current density, as will be shown in the paragraph that follows, is $\frac{qnv}{4}$ where q is the electronic charge and n is the electron number density. The collecting area of the probe is the surface area of the probe, i.e., $4\pi r_p^2$ as Fig. 3 suggests.

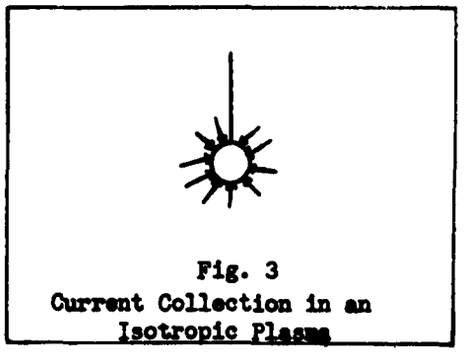

Fig. 3
Current Collection in an Isotropic Plasma

By an electron scattering approach, the current density is quite easily determined. In Fig. 4 (shown on the following page) S is a unit of area normal to the Z direction. If Σ_s represents the macroscopic electron elastic scattering cross section of the neutral gas

atoms, then the number of electrons elastically scattered out of volume element $r^2\sin\theta d\theta d\phi dr$ is $nv\Sigma_s r^2\sin\theta d\theta d\phi dr$. Not all of these electrons will reach area S since some will be attenuated en route by elastic scattering and also because the scattering is assumed to be isotropic. The number scattered out of the volume element and reaching S is thus $\frac{nv\Sigma_s r^2 e^{-\Sigma_s r}}{4\pi r^2}\sin\theta\cos\theta d\theta d\phi dr$. The fact that some electrons could be inelastically scattered is ignored because for most values that v will assume, the macroscopic inelastic scattering cross section is small. The current density J striking S from the positive Z direction is therefore given by

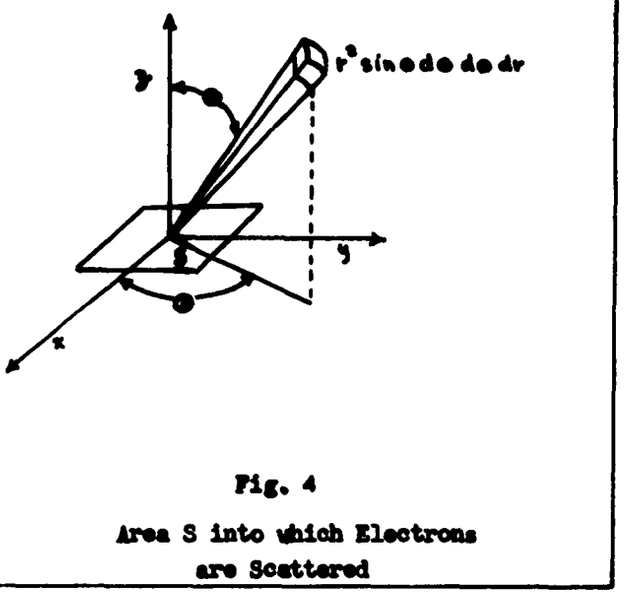

Fig. 4
Area S into which Electrons are Scattered

$$J = \int_0^r \int_0^{2\pi} \int_0^{\frac{\pi}{2}} \frac{nv}{4\pi} \Sigma_s e^{-\Sigma_s r} \cos\theta\sin\theta d\theta d\phi dr \qquad (12)$$

If it is assumed that the area S is far from the boundaries of the plasma, the upper limit of r may be set at infinity. Therefore

$$J = \int_0^{\infty} \int_0^{2\pi} \int_0^{\frac{\pi}{2}} \frac{qnv}{4} \Sigma_s e^{-\Sigma_s r} \cos\theta \sin\theta d\theta d\phi dr \tag{13}$$

and upon integration

$$J = \frac{qnv}{4} \tag{14}$$

Since I, the probe current is the product of the collecting area and the current density

$$I = \frac{4\pi r_p^2 qnv}{4} \tag{15}$$

or

$$I = \pi r_p^2 qnv \tag{16}$$

Probe Collection of a Parallel Swarm of Monoenergetic Electrons

If the same spherical probe is placed in a mono-directional parallel swarm of monoenergetic electrons, Fig. 5, and the probe potential is the same as plasma potential the current collected by the probe is again equal to the product of the collecting area and the current density which are now different from the

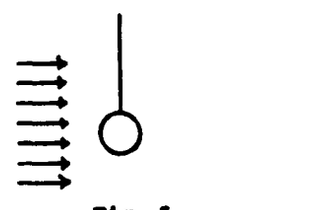

Fig. 5
Current Collection in a Parallel Swarm of Electrons

isotropic case. The collecting area for the parallel swarm is the cross-sectional area of the probe (Fig. 5 on the preceding page), i.e., πr_p^2. The current density is qnv. Thus,

$$I = \pi r_p^2 qnv \tag{17}$$

This is the same equation as Eq (16). Hence, a spherical probe in a plasma of monoenergetic electrons can be analyzed as a spherical probe in a monoenergetic parallel swarm of electrons. By further extension of this idea a spherical probe in any plasma can be analyzed as a spherical probe in many parallel swarms of electrons in which each parallel swarm corresponds to a particular energy range.

Effect of Probe Potential on Effective Collecting Area

If a potential is applied to the probe that is negative with respect to plasma potential, the electrons will be repelled from the probe. If a positive potential is applied with respect to the plasma potential, the electrons will be attracted to the probe. Their behavior, when in the presence of the probe, can best be examined by considering a monoenergetic parallel swarm of electrons and by determining their impact parameters. The impact parameter of an electron in the presence of the probe is the distance by which the electron would miss the center of the probe if there were no Coulomb force between them. The impact parameter for grazing incidence on the probe is the impact parameter of an electron which just touches the surface of the probe as it passes by the probe.

If p_g represents the impact parameter for grazing incidence on the probe, then electrons with impact parameter less than p_g will be collected by the probe and electrons with impact parameters greater than p_g will not be collected. Figure 6 illustrates two situations. Fig. 6a is the case of electron acceleration, i.e., $V > 0$ where V is the potential of the probe referenced to plasma potential. Figure 6b is the case of electron retardation, i.e., $V < 0$. The different paths the electrons assume in the two cases is due, of course, to the Coulomb force between the electrons and the probe. In a parallel swarm of electrons, if the probe is at a potential other than plasma potential, the collecting area will not be the cross-sectional area of the spherical probe but will be a function of p_g specifically πp_g^2. As Fig. 6 indicates, in the case of a probe potential negative with respect to plasma potential, the collecting area is less than the cross-sectional

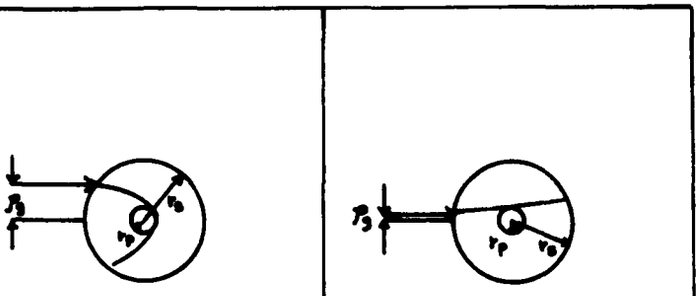

Fig. 6
Impact Parameters for Grazing Incidence
(From Ref 11:2512)

area of the probe since $p_g < r_p$. In the case of the probe at a potential positive with respect to the plasma, the collecting area is greater since $p_g > r_p$. An equation for probe current in a monoenergetic parallel swarm of electrons for a spherical probe at any potential may again be written as the product of the collecting area and current density. The collecting area of the probe for probe potentials other than plasma potentials is πp_g^2 within limitations which will be discussed on page 25. The current density is again qnv. Therefore,

$$I = \pi p_g^2 qnv \tag{18}$$

which, following the reasoning used previously, is not only the equation for current collection in a monoenergetic parallel swarm of electrons, but is also the equation for current collection in a plasma of monoenergetic electrons.

Calculation of p_g

p_g may be calculated as a function of probe radius, probe potential, and electron energy by considering the equations of conservation of energy and conservation of angular momentum about the probe and by assuming the potential drop between probe and plasma occurs across the sheath.

By the law of conservation of energy, the kinetic energy of an electron at the probe equals the sum of the kinetic energy of the electron at the sheath and its potential energy, i.e.,

$$\frac{1}{2} mv_p^2 = \frac{1}{2} mv_s^2 + qV \tag{19}$$

where v_p is the velocity of the electron at probe;

v_s is the velocity of the electron at sheath.

v_p, however, is composed of radial and tangential components to the probe, i.e.,

$$v_p^2 = v_{rp}^2 + v_{tp}^2 \tag{20}$$

where v_{rp} is the radial component of velocity at probe;

v_{tp} is the tangential component of velocity at probe.

v_{rp}, however, must equal zero in order for an electron to graze the probe. Thus,

$$v_p^2 = v_{tp}^2 \tag{21}$$

Substituting Eq (21) into Eq (19)

$$\frac{1}{2} mv_{tp}^2 = \frac{1}{2} mv_s^2 + qV \tag{22}$$

Since angular momentum about the probe must be conserved, the angular momentum of the electron at the sheath must equal the angular momentum at the probe.

$$r \times mv_s = r_p \times mv_p \tag{23}$$

For grazing incidence at the probe,

$$p_g mv_s = r_p mv_{tp} \tag{24}$$

and thus,

$$v_{tp} = \frac{p_g v_s}{r_p} \tag{25}$$

Substituting Eq (25) into Eq (22) yields

$$\frac{1}{2}m\frac{p_g^2 v_s^2}{r_p^2} = \frac{1}{2}mv_s^2 + qV \tag{26}$$

Dividing Eq (26) by $\frac{1}{2}\frac{mv_s^2}{r_p^2}$ yields

$$p_g^2 = r_p^2 + \frac{2r_p^2 qV}{mv_s^2} \tag{27}$$

or

$$p_g^2 = r_p^2\left(1 + \frac{qV}{E}\right) \tag{28}$$

where E is the energy of the electron at the sheath edge which is the energy of the electron in the undisturbed plasma. Equation (28) may also be written as

$$p_g^2 = r_p^2\left(1 + \frac{V}{U}\right) \tag{29}$$

where U is the kinetic energy of the electron in electron volts.

p_g for the Positive and Negative Probe

At this time it is worthwhile to examine Eq (28) in terms of Fig. 6. When the potential of the probe is more positive than plasma potential, p_g is greater than r_p for all energies. Equation (28) demonstrates that p_g at a fixed potential approaches infinity for energies approaching zero. This is not logical except in the case of the probe with an infinite sheath. Since the potential drop between probe and plasma is assumed to occur across the sheath, only those electrons reaching the sheath, i.e., those with $p_g = r_s$, are attracted to the probe. Therefore in the electron-accelerating region the upper limit of p_g equals r_s. Thus for $0 < E < E_k$, p_g must equal r_s. Substituting $p_g = r_s$ into Eq (28)yields

$$r_s^2 = r_p^2\left(1 + \frac{qV}{E_k}\right) \tag{30}$$

Therefore,

$$E_k = \frac{qV}{\left[\frac{r_s}{r_p}\right]^2 - 1} \tag{31}$$

The region of interest in determining electron energy distributions, however, is for probe potentials less than plasma potential.

When the potential of the probe is less than plasma potential p_g is indeed less than r_p for $|qV| \leq E < \infty$ as Eq (28) indicates. Thus the collecting area is less than the cross-sectional area. The limits

are set on E since an infinitely fast electron has a grazing impact parameter $p_g = r_p$ while an electron with energy $E = |qV|$ has a grazing impact parameter $p_g = 0$. Electrons with $E < |qV|$ will not be collected by the probe.

Derivation of General Current Equation in Electron Retarding Region

By substituting Eq (28) into Eq (18), Eq (18) may now be written as

$$I = \pi r_p^2 (1 + \frac{qV}{E}) qnv \tag{32}$$

where V will be restricted to values negative with respect to plasma potential. Converting Eq (32) to a function of energy,

$$I = \pi r_p^2 qn (\frac{2}{m})^{1/2} (1 + \frac{qV}{E}) E^{1/2} \quad \text{for} \quad V < 0 \tag{33}$$

General energy distributions may now be considered by superposition of infinitesimal monoenergetic contributions. If $F(E)$ is defined as the fraction of electrons per unit energy interval, then $F(E)dE$ is the fraction of electrons with energies between E and $E + dE$ and $nF(E)dE$ is the number density with energies between E and $E + dE$. The contribution to the probe current for an energy range from E to $E + dE$ is therefore

$$dI = \pi r_p^2 qn (\frac{2}{m})^{1/2} (1 + \frac{qV}{E}) E^{1/2} F(E) dE \quad \text{for} \quad V < 0 \tag{34}$$

Since Eq (34) is restricted to probe potentials negative with respect to plasma potential the total current at a particular potential may be

found by integrating Eq (34) over all energies of electrons that can be collected by the probe. For a particular $V < 0$ the lowest energy electron that may be collected is E_V, where E_V approaches qV as a limit, i.e., $\lim_{\Delta E \to 0} (E_V + \Delta E) = qV$. Thus

$$I = K\int_{E_V}^{\infty} (1 + \frac{qV}{E})E^{1/2}F(E)dE \tag{35}$$

where $K = \pi r_p^2 qn(\frac{2}{m})^{1/2}$.

Derivation of Electron Energy Distribution Function

By differentiating Eq (35) twice, it will now be shown that the distribution function can be expressed in terms of the second derivative of probe current with respect to probe voltage.

$$\frac{dI}{dV} = K\int_{E_V}^{\infty} (\frac{q}{E})E^{1/2}F(E)dE \tag{36}$$

and

$$\frac{dI}{dV} = Kq\int_{E_V}^{\infty} E^{-1/2}F(E)dE \tag{37}$$

Since E_V approaches qV as a limit

$$dE_V = qdV \tag{38}$$

$$\frac{dI}{dE_V} = \frac{1}{q}\frac{dI}{dV} \tag{39}$$

$$\frac{d^2I}{dE_V^2} = \frac{1}{q}\frac{d\left(\frac{dI}{dV}\right)}{dE_V} \tag{40}$$

Substituting Eq (38) into Eq (40) yields

$$\frac{d^2I}{dE_V^2} = \frac{1}{q}\frac{d\left(\frac{dI}{dV}\right)}{qdV} \tag{41}$$

and

$$\frac{d^2I}{dE_V^2} = \frac{1}{q^2}\frac{d^2I}{dV^2} \tag{42}$$

Substituting Eq (39) into Eq (37) yields

$$\frac{dI}{dE_V} = \frac{Kq}{q}\int_{E_V}^{\infty} E^{-1/2}F(E)dE \tag{43}$$

Differentiating Eq (43) with respect to E_V and simplifying yields

$$\frac{d^2I}{dE_V^2} = K(E_V)^{-1/2}F(E_V) \tag{44}$$

Substituting Eq (42) into Eq (44) yields

$$\frac{d^2I}{dV^2} = Kq^2(E_V)^{-1/2}F(E_V) \tag{45}$$

or

$$F(E_V) = K' \frac{d^2I}{dV^2}(E_V)^{1/2} \tag{46}$$

where $K' = Kq^2$.

The significance of Eq (46) is that the fraction of electrons having a particular energy E_V (where E_V approaches qV as a limit) per unit energy interval can be determined by multiplying the second derivative of probe current with respect to probe potential by the square root of the energy E_V. E_V and the second derivative of probe current can be obtained from the second derivative of a probe curve automatically plotted from data taken by a spherical probe. If Eq (46) is applied throughout the electron-retarding region the energy distribution of the electrons may be determined as will be discussed more fully in Chapter VI.

Location of Plasma Potential

The fact that plasma potential occurs at the inflection point of a probe curve will now be shown. As has been mentioned on page 25, when the probe is at a positive potential, those electrons whose energies are less than E_k will have an impact parameter for grazing incidence of $p_g = r_s$. For an infinitely thin sheath, i.e., when

$r_s \to r_p$, $E_k \to \infty$ as Eq (31) indicates. Hence when $r_s \to r_p$ electrons of all energies will have $p_g = r_s$ and the probe current for $V > 0$ is given by

$$I = \int_0^\infty \pi r_s^2 qn\left(\frac{2}{m}\right)^{1/2} E^{1/2} F(E)dE \qquad \text{for } V > 0,\ r_s \to r_p \qquad (47)$$

since the collecting area is now πr_s^2.

The above equation is independent of V; hence the current will saturate above plasma potential for the case of the infinitely thin sheath. Since $r_s \to r_p$, the value at which the current will saturate is the value of the current at plasma potential because at plasma potential $E_V = 0$ and $V = 0$ in Eq (24).

For the other extreme case of an infinitely large sheath $E_k \to 0$ in Eq (31). Since r_s is infinitely large, Eq (28) gives the correct value of p_g for all V. Thus the current is now given by

$$I = \int_0^\infty \pi r_p^2 qn\left(\frac{2}{m}\right)^{1/2}\left(1 + \frac{qV}{E}\right)(E^{1/2})F(E)dE \qquad \text{for } V > 0,\ r_s \to \infty \qquad (48)$$

Upon integration, I will be in the form of $I = a + bV$ where a and b are constants (Ref 11:2515). Since Eq (48) at $V = 0$ is the same as Eq (35) at $V = 0$ and Eq (48) is linear in V, the portion of the probe curve in the accelerating region is tangent to the probe curve in the retarding region and is linear.

Actual probes have neither infinitely thin sheaths or infinitely large sheaths. Therefore actual probe curves in the electron-accelerating region must lie between the two limiting cases, Fig. 7. Since the upper limit of the probe curve for $V > 0$ is linear and tangent to the curve for $V < 0$ the actual probe curve at most must be linear. It more probably will be concave downward, however.

The probe curve in the electron-retarding region will now be shown to be concave upward. For the monoenergetic case, it has been shown that

$$I = nvq(1 + \frac{qV}{E})\pi r_p^2 \qquad (32)$$

Thus for a constant E, I varies linearly with V. At the potential V where $E = -qV$ the current will be zero. When $V = 0$, I is at its maximum in the electron retarding region, i.e.,

$$I = nvq\pi r_p^2 \qquad (16)$$

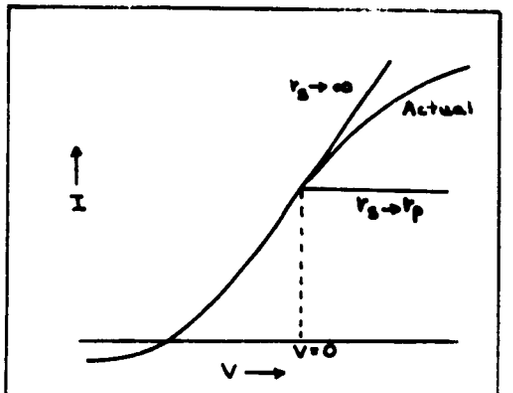

Fig. 7
Actual Probe Curve with Two Limiting Cases

If one considers a hypothetical plasma containing electrons of three energy groups E_1, E_2, and E_3 in which (a) $E_1 > E_2 > E_3$, (b) the number density of

each group is n_1, n_2, and n_3, respectively, and (c) the velocity of each group, i.e., V_1, V_2, and V_3, respectively, then a probe curve such as the one in Fig. 8 may be constructed with the use of Eq (32). This idea may be extended to a plasma containing all energies with the resulting figure concave upward. Thus plasma potential does indeed correspond to the inflection point in a probe curve since it marks the transition from a curve that is concave upward to one that is either linear or more probably concave downward. Plasma potential also must correspond to the point where the second derivative of the probe curve equals zero since the second derivative of any curve at its inflection point is zero.

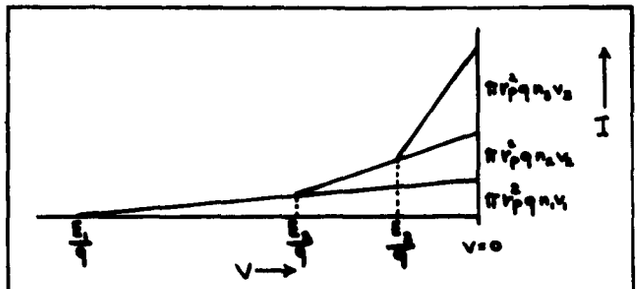

Fig. 8

Superposition of Probe Current

(From Ref 10:1243)

Calculation of Plasma Density

From Fig. 8 it can be seen that the current at plasma potential for a plasma having electrons of energies E_1, E_2, and E_3 is

given by

$$I = \pi r_p^2 q \sum_{i=1}^{3} n_i v_i \tag{49}$$

Therefore, for a plasma having N energy groups

$$I = \pi r_p^2 q \sum_{i=1}^{N} n_i v_i \tag{50}$$

But since

$$\bar{v} \equiv \frac{\sum_{i=1}^{N} n_i v_i}{\sum_{i=1}^{N} n_i} \tag{51}$$

and

$$n = \sum_{i=1}^{N} n_i \tag{52}$$

and

$$n\bar{v} = \sum_{i=1}^{N} n_i v_i \tag{53}$$

$$I = \pi r_p^2 q n \bar{v} \tag{54}$$

or

$$n = I/\pi r_p^2 q \bar{v} \tag{55}$$

Therefore, if the radius of the probe and the current at plasma potential are known, plasma density may be calculated by first computing the average electron velocity and then using Eq (55).

V. Equipment

The following steps were undertaken by the author in preparing the equipment for data taking:

(1) Design, construction and mounting of the plasma tube;

(2) "Bake-out" of the tube and subsequent filling with argon;

(3) Installation of the plasma exciting equipment;

(4) Installation of the measuring equipment;

(5) Positioning of the probe along the axis of the exciting coil;

(6) Cleaning of the probe.

Plasma Tube

The tube that contained the plasma is shown in Fig. 9 on the following page. The tube was 11.5 cm in diameter and 20.5 cm high. It was designed with a champagne bottle shape on both ends to prevent collapsing at high vacuums. The tube and the entire system were tested with a helium leak detector at a vacuum of 10^{-6} torr and no leaks were found.

Since there is no physical way in which to reference a probe to a plasma directly, a reference electrode must be located in the plasma for all probe measurements. For a DC plasma the probe may be referenced to one of the electrodes already in the tube, i.e., the anode or

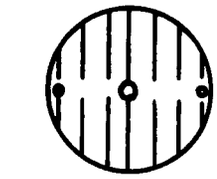

Reference Electrode

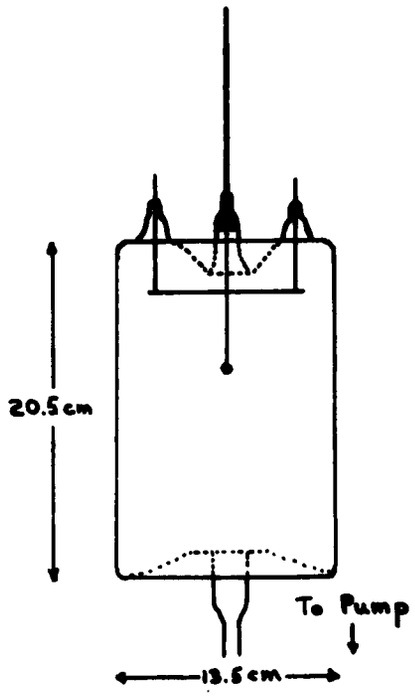

Fig. 9

Plasma Tube

cathode. For an electrodeless discharge (RF excited plasma) a reference electrode must be placed in the tube.

The reference electrode, Fig. 9, used in this experiment was a 10-cm-in-diameter circular Monel disk 0.5 mm thick. Monel was chosen because it is easy to work with and is non-magnetic. The rather large size of the reference electrode was selected for two reasons. First, it was easier to construct than a smaller one would be. Secondly, Fetz and Oechsner (Ref 4:251) recommended in their paper on the determination of plasma potential of an RF excited plasma that the ratio of surface area of the reference electrode to the surface area of the probe be at least 1000:1. The ratio in this case was 22,000:1.

The physical reason for the large ratio between probe and reference electrode area is obvious. When the probe draws electrons from a plasma, the reference electrode draws an equal number of positive ions. If the reference electrode were the same size as the probe, when the potential between probe and plasma is made more positive, the probe would only draw an increasing amount of electron current until ion saturation of the reference electrode occurred. When ion saturation of the reference electrode is reached, electron saturation of the probe must be reached because the probe cannot remove more electrons from the plasma than the reference electrode can remove ions. In examining the typical probe curve in Fig. 2, it is evident that ion saturation of the reference electrode would distort the shape of the electron current of the probe drastically. If the reference electrode is made many times larger than the probe, the reference electrode will then increase its ion collecting

capability by a factor approximating the ratio of the reference electrode area to the area of the probe. If this is done, the reference electrode will not saturate before electron saturation of the probe occurs and hence will have no effect on the electron drawing capability of the probe.

A 1-cm-in-diameter hole was cut in the center of the reference electrode to allow the probe to pass through. The two rows of seven 0.1-cm-wide evenly spaced slits in the reference electrode (Fig. 9) were cut for the purpose of preventing eddy currents. Spot welded to the reference electrode were two 0.1-cm inside diameter Monel sleeves 7 cm apart. Into each sleeve was fitted a Kovar wire, 8 cm long and 0.1 cm in diameter. These two wires suspended the reference electrode in the bottle and protruded 1 cm through the glass tube to provide electrical contacts so that the probe could be referenced to ground.

The probe consisted of a 0.54-mm-in-diameter tungsten sphere suspended on a tungsten wire. Surrounding the wire was a quartz capillary to prevent electrons and ions from being collected by the wire in addition to being collected by the probe. The probe was designed to be capable of being raised to within 2.5 cm of the reference electrode and lowered to 9 cm from the reference electrode.

The plasma tube was blown by the glass blower of the Electronic Technology Laboratory and mounted on a pump stand. Figure 10, shown on the following page, is a schematic showing the placement of the tube on the pump stand and the valve arrangement used for filling the tube.

Vacuum System

The argon gas that was used to fill the plasma tube used in this investigation was supplied by the 1.1 liter bottle shown below in Fig. 10. This bottle was connected to the system by the 2-cm-in-diameter glass tube 21.1 cm long which extended from the bottle to a Kovar seal which connected the glass tubing to a Kovar tube 0.2 cm in diameter and 17 cm long. This thin Kovar tube was connected to valve 3.

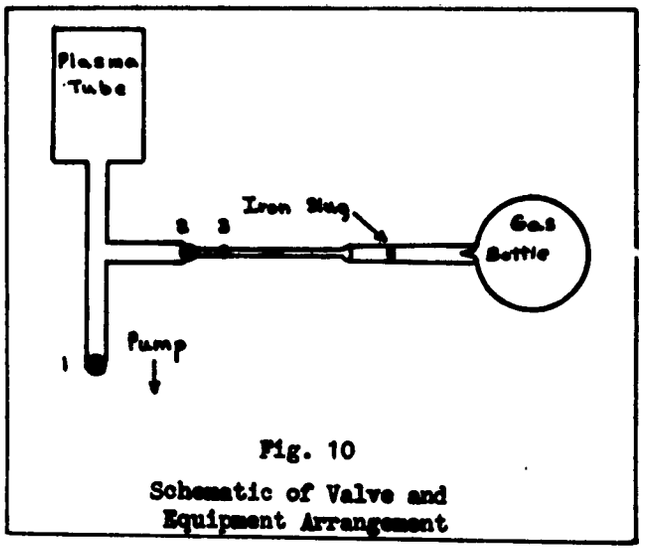

Fig. 10
Schematic of Valve and Equipment Arrangement

The bottle was sealed by the manufacturer by means of a glass tip as seen at the junction of the glass tubing and gas bottle in Fig. 10. In order to allow the gas to escape, this tip had to be broken. Before the glass tube was sealed to the Kovar tube, an iron slug was placed in the glass tube. This slug was moved up against the glass tip (at the appropriate time) by means of a magnet until the tip broke. To insure a clean system, this iron slug must be encapsulated in glass before it is inserted into the glass tubing in order to eliminate outgassing from the slug.

Valves 1, 2, and 3 were designed by the Electronic Technology Laboratory for high vacuum work. They have the characteristic of being able to hold a vacuum of 10^{-8} torr and can withstand at least 120 "bake-outs".

To insure an impurity-free system, the tube, valves, and connecting pipes had to be baked before the tube was filled with argon. Valves 1, 2, and 3 were opened, the pumps were put in operation, and an electrical oven was lowered over the equipment. The tube was baked for 10 hours at 450°C until all outgassing ceased. The oven was raised, all valves were closed, and the iron slug was then rammed up against the glass tip, breaking it and allowing gas to fill the glass tubing. Valve 3 was opened and then closed again to allow gas to fill the volume between valve 3 and 2. Valve 2 was then opened, allowing gas to fill the plasma tube.

Exciting Coil

The plasma-exciting coil used in this investigation was a one-turn copper coil 16.5 cm in diameter. The copper coil was made by bending a 52 × 17.7 × 0.2 cm sheet of copper in the form of a cylinder. The ends, however, were not completely closed. A gap of 1.5 cm remained and the two ends of the copper coil were bent perpendicular to the coil surface to create two 0.75-cm-wide flaps as shown in Fig. 11 on the following page. This was done so that a variable mica capacitor could be placed across the coil and to provide a convenient place to attach the power input coils. One RG-8/U shielded coaxial cable was bolted and soldered

to each side of the coil at the slit to provide the power leads to the coil. The tank circuit consisting of the variable capacitor and the copper coil was tuned to the transmitter frequency, which was 21.3 mc. This frequency was selected because it lies in the amateur band and because its associated wavelength is large compared to the dimensions of the coil, i.e., the ratio of wavelength to coil circumference is about 30 to 1. Because of this fact and the fact that the coil was fed push-pull, the current at any point on the coil at any instant of time was constant; hence, the field at the center of the coil was zero and the ground plane mentioned in Chapter II existed in the tube.

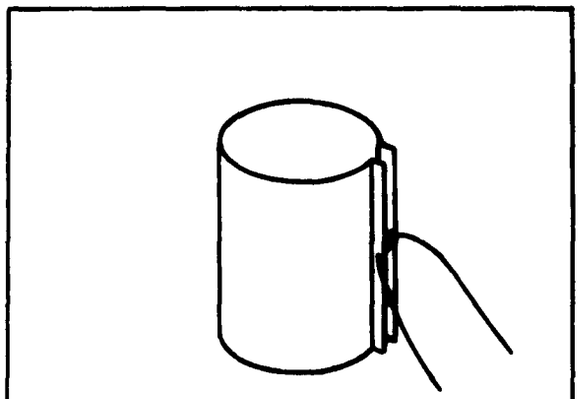

Fig. 11

Plasma Exciting Coil

Power Source

The transmitter used as a source of power in exciting the plasma was a commercial Viking Ranger made by E. F. Johnson Company. It had a single-ended output rated at 65 watts. The RF power was fed by an RG-8/U coaxial cable to a T-splice contained inside a grounded aluminum

box. The output cables from the T-splice were the ones bolted and soldered to the coil in Fig. 11, as mentioned. The lengths of the coaxial cables were 0.65 meters and 5.30 meters.

The physical length of wire corresponding to a half wave length of current or voltage is given by

$$\lambda = \frac{C}{2\nu} \times VF \tag{56}$$

where λ = physical wave length of wire

C = velocity of light in free space

VF = velocity factor which is defined as the ratio of wavelength in wire to wavelength in free space

ν = frequency of operation.

For RG-8/U the velocity factor is 0.66 (Ref 15:348).

Hence,
$$\lambda = \frac{3 \times 10^8}{2 \times 21.3 \times 10^6} \times .66 \tag{57}$$

$$\lambda = 4.65 \text{ mtrs} \tag{58}$$

The two coaxial cables used, therefore, differed in length by one-half wavelength. Thus at any instant of time the current and voltage at the coil end of one cable were 180° out of phase with the current and voltage at the coil end of the other cable. By this judicious selection of lengths, the single-ended feed of the transmitter was converted to

push-pull. This arrangement for converting from single-ended to push-pull feed was adopted because of expediency. Another arrangement which will be mentioned in the following paragraph did not work satisfactorily.

An attempt was made to feed the single-ended output of the transmitter to the primary of a transformer having a center-tapped secondary in order to convert the single-ended feed to push-pull. A good impedance match could not be made and the resulting plasma was so weak that probe curves could not be taken. A laboratory-built generator (not designed for this experiment) with a push-pull output was tried, but it had no RF ground. Balanced amounts of power could not be fed from this transmitter into each side of the coil since the oscillator was self-exciting. In this case the plasma was quite dense, but a large amount of RF interference was picked up by the probe so that the condition of no RF potential between probe and plasma could not be met; hence, no meaningful probe curves could be taken. The author started building a crystal controlled oscillator having a push-pull power output, but due to time limitations was unable to complete it. A push-pull transmitter is more desirable for an experiment of this nature, but it is not absolutely necessary if one is not available.

Probe Circuit

Schematically the circuitry for plotting of probe curves is as shown in Fig. 12 on the following page. R_j, the voltage dropping resistor, must be small in comparison to the apparent impedance of

the plasma R_p so that the sweep potential will be the potential that appears between probe and plasma, i.e.,

$$E_s = I \times (R_p + R_j) \approx I \times R_p \tag{59}$$

This is necessary so that for every value of probe current the corresponding value of probe voltage will be known accurately. Values of 5, 10, and 500 ohms were used for R_j to meet this requirement.

The voltage across R_j is the input to the Y axis of an X-Y plotter and the voltage of the variable sweep supply is the input to the X axis of the plotter. As the power supply is swept manually through various potentials of the probe with respect to the reference electrode, the plotter will automatically plot the voltage across R_j (which is proportional to probe current) versus the probe potential.

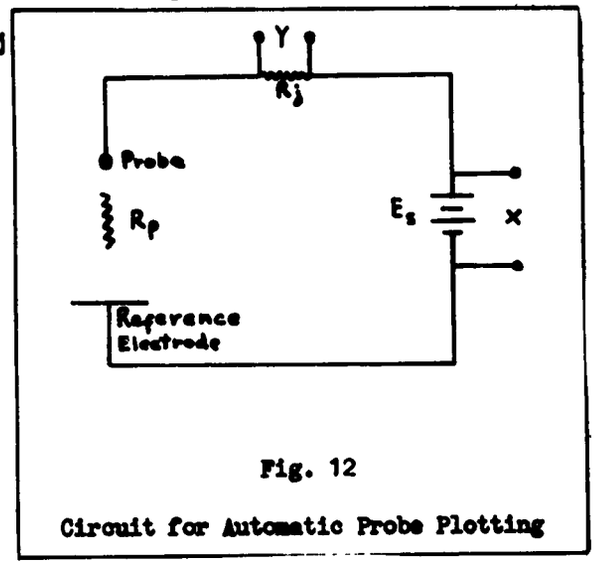

Fig. 12

Circuit for Automatic Probe Plotting

In this investigation an instrument designed by the Electronic Technology Laboratory was used in taking probe curves. It not only plotted probe curves using an X-Y plotter, but also had the capability of plotting with the same X-Y plotter the second derivatives of the

probe curves; hence, it will be referred to as the Second Derivative Apparatus.

To take second derivatives the Second Derivative Apparatus superimposes a very small pure 1-kc sinusoidal signal on the DC probe voltage which is swept manually. In this investigation a 40 mv signal was used. The second harmonic in the probe current caused by the nonlinearity of the probe curve is filtered, amplified, rectified by a phase true detector, and plotted by the X-Y plotter. The second harmonic is proportional to the second derivative of probe current with respect to probe voltage. A more detailed description of the Second Derivative Apparatus may be found in an article published in the March, 1963, issue of the Review of Scientific Instruments (Ref 9).

Grounding and Shielding of Equipment

Special effort was taken in grounding and shielding the test apparatus. The transmitter chassis, the aluminum box containing the T-splice, the reference electrode, the electrical center of the exciting coil, and the outer conductors of the coaxial cables were all tied into a common ground. The radiating sources of RF power such as the transmitter, the power leads, and the T-splice were shielded so that the RF power fed into the plasma would be only that fed in by the exciting coil and hence would be introduced symmetrically. The Second Derivative Apparatus was shielded by its chassis, and its chassis was grounded.

Equipment Layout

The layout of the equipment as used in this experiment is shown in Fig. 13 on the following page. The large instrument in the left foreground is the Second Derivative Apparatus. Centered in the picture is the glass tube which contained the plasma. The probe shaft is seen protruding from the top. Surrounding the tube is the one-turn, copper coil used to excite the plasma, and to its right is the aluminum box which contained the T-splice used in changing the transmitter's single-ended feed to push-pull feed. The instrument to its rear with the large dial in the center and the smaller dial in the upper right-hand corner is the Viking Ranger RF transmitter. The large hexagonal object in the center of the upper part of the picture is the oven used to bake the tube. Figure 14 on page 47 is a close-up of the tube and excitation coil. The coaxial cable fastened to the probe and reference electrode by the alligator clips leads to the Second Derivative Apparatus. The glass bottle containing the filling gas may be seen in the right rear. Valves marked 2 and 3 in Fig. 10 may be seen in the right foreground standing upright on the thin Kovar tubing coming from the bottle containing the filling gas.

Before taking probe curves, two tasks remained to be accomplished. First, the exciting coil had to be centered around the plasma tube so that the probe would be in the field-free region and so that no RF potential would exist between probe and plasma. Secondly, the probe had to be cleaned by sputtering before taking probe curves.

Fig. 13

Equipment Layout

Fig. 14

Plasma Tube and Exciting Coil

Centering of Coil

The centering of the coil was verified by the circuit in Fig. 15. The variable supply E_b consisted of batteries in series to give potentials between the probe and reference electrode of 0, 11, 12, 14.5, 22, and 29 volts. Thus points along the probe curve from the ion region to the electron accelerating region could be examined. A floating DC sweep supply was not used because it was felt that any RF might be bled off to ground through the DC supply before reaching the 10 ohm resistor. A 0.004 μf RF by-pass capacitor was placed across the terminals of the battery to provide a low impedance path for the RF. At the frequency of operation the impedance of the capacitor is less than 2 ohms. The batteries, the by-pass capacitor, and the 10 ohm resistor were placed in an aluminum box, as indicated by the dotted line in Fig. 15, to prevent RF pickup. All leads into and out of the box were shielded.

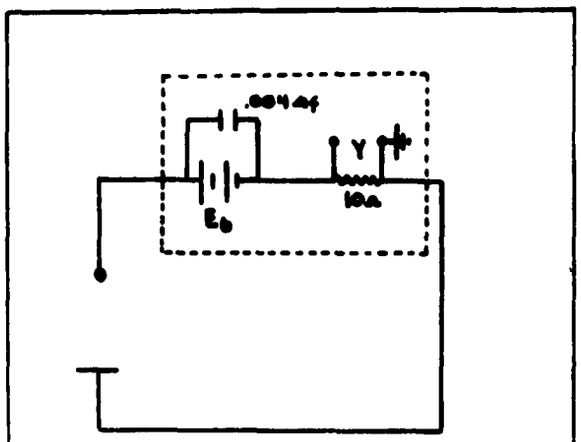

Fig. 15

Circuit for Detection of RF on Probe

The voltage drop across the 10 ohm resistor was fed into the Y axis of a Tektronix Type 545 oscilloscope. The X axis was swept

internally. The coil was first centered about the probe visually. At potentials of 0, 11, and 12 volts, no RF appeared on the scope with the vertical axis set at its maximum sensitivity, i.e., 1 mv per inch. At 14.5 volts a small but detectable amount was observed, i.e., about 0.25 mv peak-to-peak voltage. When the coil was adjusted slightly the RF was eliminated for all bias voltages up to 29 volts.

Cleaning of Probe

The probe was cleaned before data taking by sputtering. The probe was made very strongly negative with respect to the plasma. The positive ions thus severely bombarded the probe, causing the surface of the probe to be eroded away. The probe was sputtered with a 200-volt negative potential for 30 seconds on two separate occasions. In addition, in order to supply additional electrons to light the discharge, a Tesla coil was placed in contact with the probe shaft. This caused the probe to become strongly negative with respect to the plasma so that each time the plasma was ignited the probe was effectively sputtered.

VI. Results and Conclusions

The Two Plasma Modes

The plasma had two steady state modes of operation. In what will be called the weak plasma the percentage of ionisation was so low that a 500-ohm voltage dropping resistor was used in order to take a probe curve. The value of the probe current drawn at plasma potential for the probe 6.3 cm from the reference electrode was 11 microamps. At this position plasma potential occurred at about 22.5 volts above ground potential, Fig. 16 as shown on the following page. Using Eq (59)

$$22.5 = 11 \times 10^{-6} \times (R_p + 500) \tag{60}$$

$$R_p = 2.2 \times 10^6 - 500 \times 2.0 \times 10^6 \text{ ohms} \tag{61}$$

Thus, the voltage dropping resistor is small compared to the impedance offered the circuit by the plasma, and, therefore, the sweep potential (in this case 22.5 volts) is the potential that appears between the probe and plasma. Unfortunately, the current drawn for the weak plasma was too small a value for the Second Derivative Apparatus and no second derivative curves could be taken in this mode of operation.

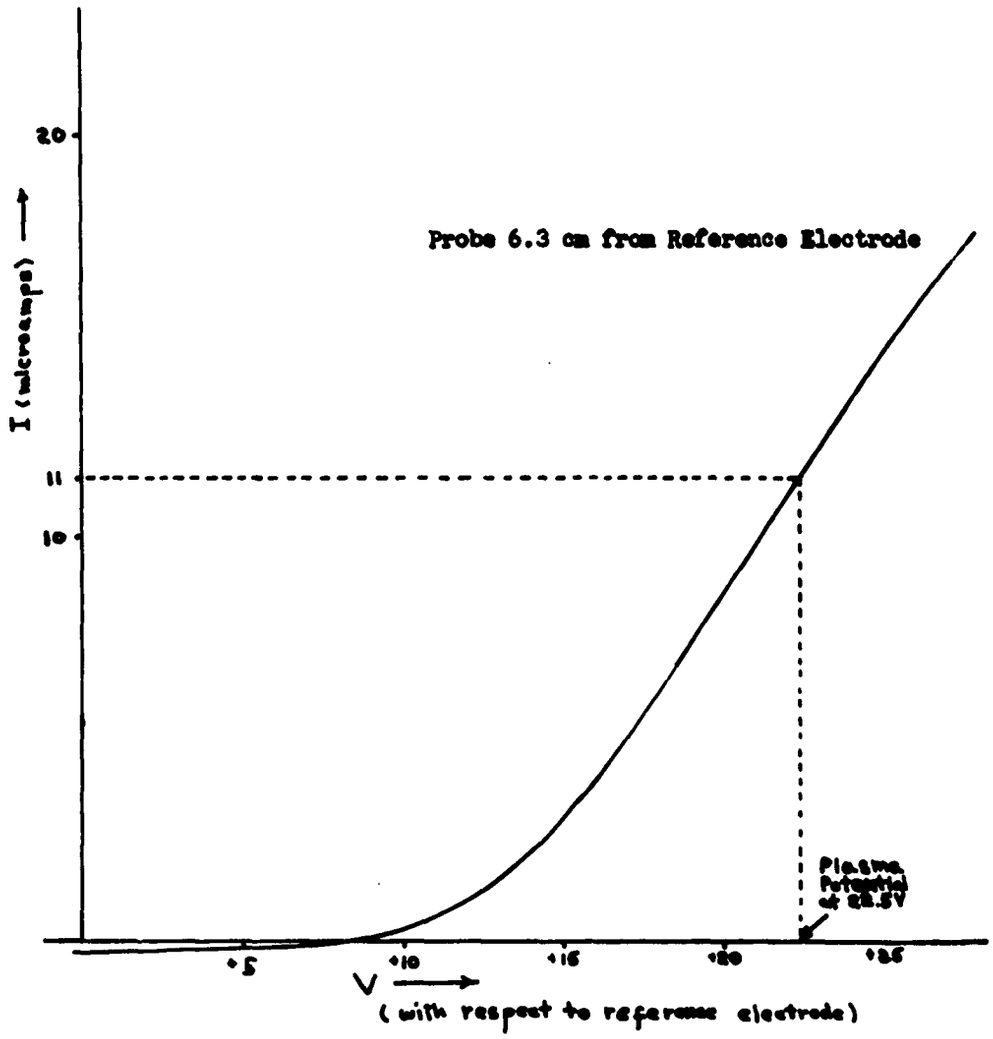

Fig. 16

Probe Curve of Dim Mode

The second mode of operation of the plasma was considerably brighter in appearance indicating a higher degree of ionisation and excitation than in the weak mode. The denser mode was achieved by putting a Tesla coil in contact with the probe shaft while the plasma was in the weak mode. This produced an additional source of electrons which in turn increased ionisation.

Plasma potential at 6.3 cm from the reference electrode for this mode occurred at about 14 volts above ground potential (Fig. 17 on the following page). The current drawn at plasma potential was 1.4 milliamps. Since the current was relatively large, a 5-ohm voltage dropping resistor was used in plotting the probe curve and the Second Derivative Apparatus was able to take the second derivative of the probe curve. The second derivative curve is shown in Fig. 18 on page 54.

A rough idea of how the energy distribution differs in the two modes of operation may be obtained by examining the two probe curves without recourse to their second derivatives. The fact that plasma potential is at a higher potential with respect to the reference electrode in the weak plasma than in the dense plasma suggests that higher energy electrons are collected by the probe in the weak plasma than in the dense plasma.

From this fact it is logical to assume that in the vicinity of the probe the electric field is stronger in the weak plasma than in the dense plasma since the local value of the electron energy is fixed by the local value of E (Ref 3:2784). This would suggest then that as the plasma becomes more ionized it has a tendency to shield

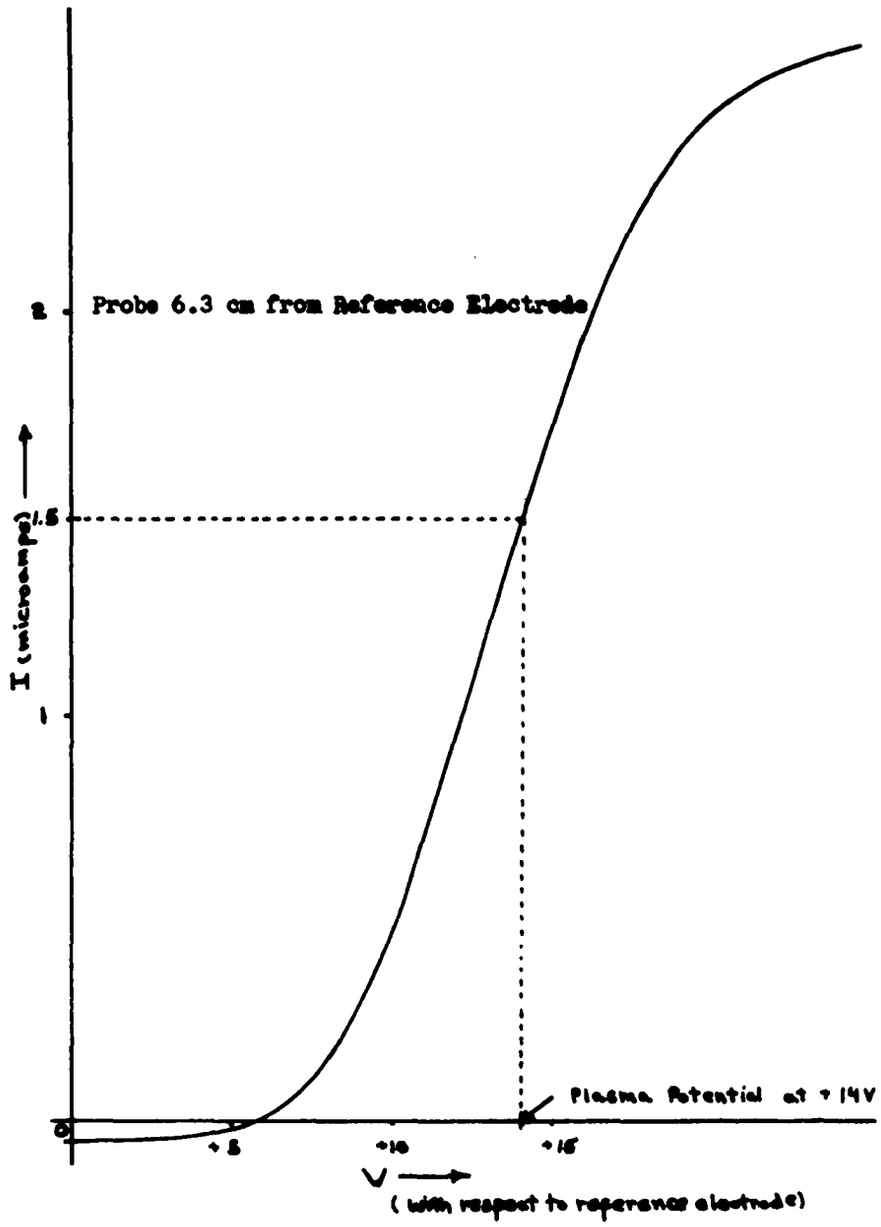

Fig. 17

Probe Curve of Dense Plasma

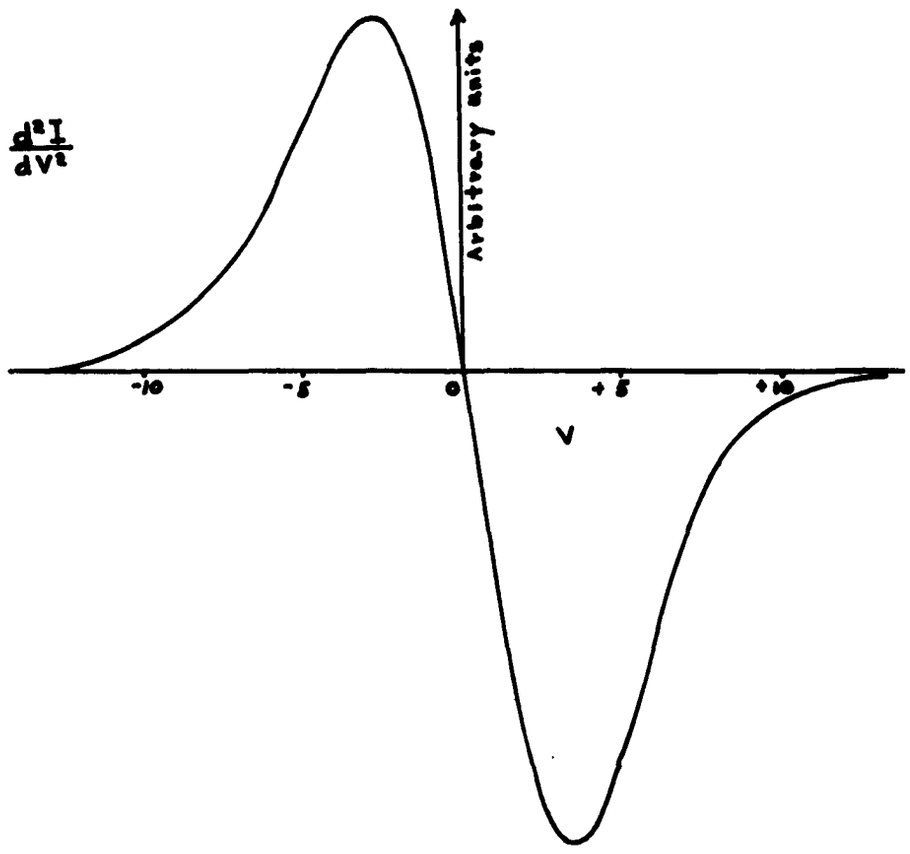

Fig. 18

Second Derivative Curve for Probe at
6.3 cm from Reference Electrode

out the RF field. This effect known as skin effect has been investigated by Eckert (Ref 3:2788). As the conductivity of the plasma increases, the radial distribution of electric field intensity changes (qualitatively) from a plot indicated by Fig. 19a to a plot indicated by Fig.19b.

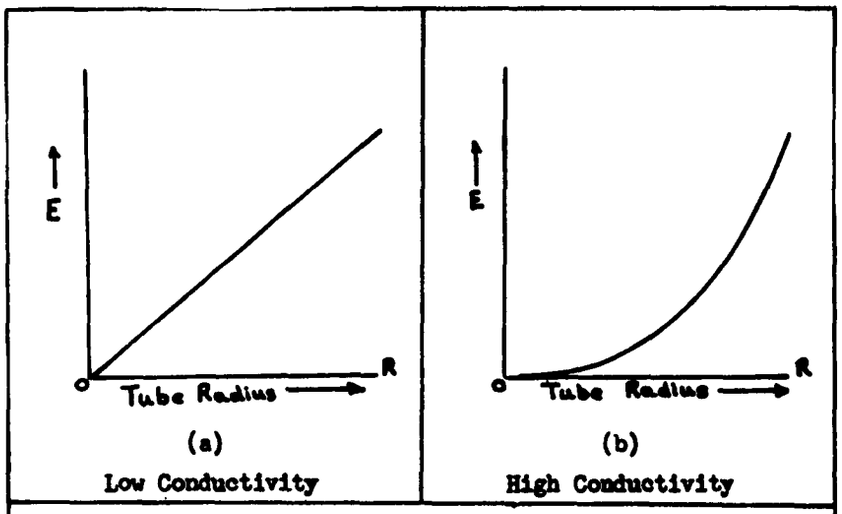

Fig. 19

Distribution of Field in Plasma

(From Ref 3:2788)

Results of Measurements in the Dense Plasma

Probe curves and their second derivatives for the dense plasma were taken for the probe at 2.5, 3.8, 5.1, 6.3, and 8.9 cm from the reference electrode. The probe did not move freely in the tube; hence probing along the axis of the tube at equally spaced increments was not possible. The second derivative for the probe 2.5 cm from the

reference electrode is shown in Fig. 20a on the following page. The resultant energy distribution curve and a Maxwellian having the same average energy are shown in Fig. 20b. Plasma potential occurs where the second derivative curve (Fig. 20a) crosses the X axis. The probe voltage with respect to the plasma is zero at this point. To the left of this point is the electron retarding region, the region of interest. The ordinates for the energy distribution curves were obtained by multiplying each ordinate of the second derivative curve in the electron retarding region taken at 0.1 ev intervals times the square root of the corresponding abscissas. Thus Eq (46) was applied throughout the electron retarding region to obtain the energy distribution spectrum. The constant K' was ignored in the calculations because at this stage of the calculations, n is not known. Thus the ordinates of $F(E)$ may be found but may not be normalized using Eq (46).

Since these calculations are rather tedious when done by hand for several probe positions in the tube, a computer program, which may be found in Appendix A, was written to accomplish this. This program automatically adjusts the RF distribution ordinates so that the data may be used to plot a normalized distribution curve. The program also computes the average energy of the electrons, their average velocity, the density of the plasma and the ordinates of a Maxwellian Distribution having the same energy as the average energy of the RF distribution.

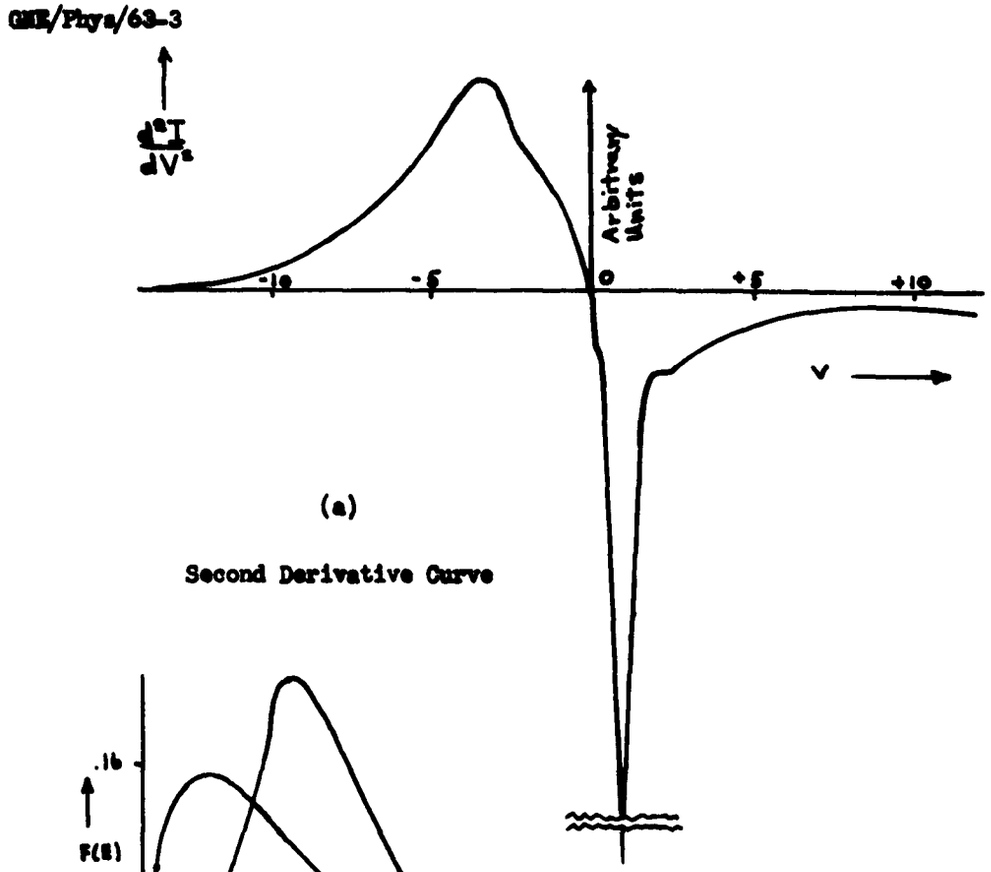

(a)

Second Derivative Curve

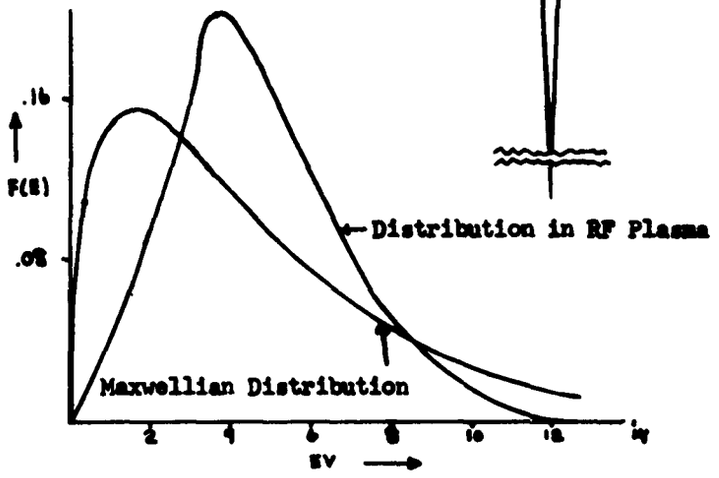

(b)

Energy Distribution Curve

Fig. 20

Second Derivative Curve and Energy Distribution Curve for Probe at 2.5 cm from Reference Electrode

Plots of the electron energy distribution for the probe at 3.8, 5.1, 6.3, and 8.9 cm from the reference electrode may be found in Fig. 21 (page 59) and Fig. 22 (page 60). Plotted with each RF distribution curve is a Maxwellian curve having the same average energy. Semi-log plots of the second derivative curves may be found in Appendix B. Since the semi-log plot of the second derivative of a Maxwellian energy distribution function is linear, these curves provide an additional means of examining the deviations of the RF electron energy distribution from a Maxwellian.

In examining Figs. 20b, 21, and 22 several facts become apparent. First, the energy distribution curves, although varying in average energy, have generally the same shape for the probe at all positions except at 2.5 cm. The proximity of the probe to the reference electrode at 2.5 cm probably accounts for the distortion noted at this position. Secondly, the curves deviate markedly from Maxwellian curves. This is to be expected since a Maxwellian is only anticipated when the particles are in thermal equilibrium and there is no external field (Ref 6:24). The low energy electrons found in Maxwellian distributions are missing from the RF distribution. This is to be expected because the RF field penetrates the plasma and removes the low energy electrons by giving them additional energy. The high energy electrons are missing because in the vicinity of the probe the accelerating electric field must be low (Fig. 19) and also because the higher energy electrons lose their energy by inelastic collisions. There are two metastable states of argon occurring at 11.5 and 11.7 ev (Ref 16:39). Thus electrons

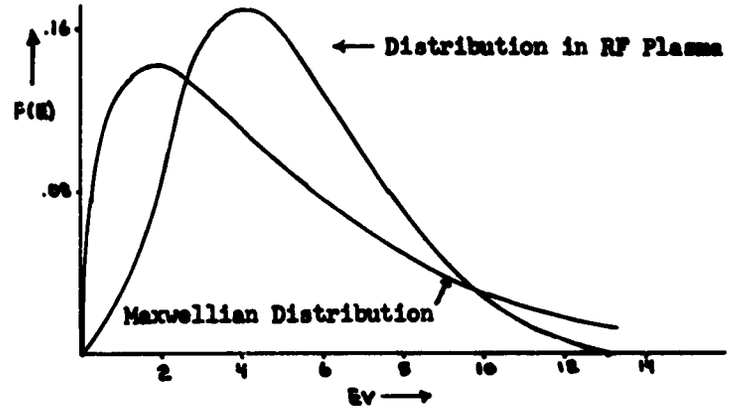

(a)

Probe at 3.8 cm from Reference Electrode

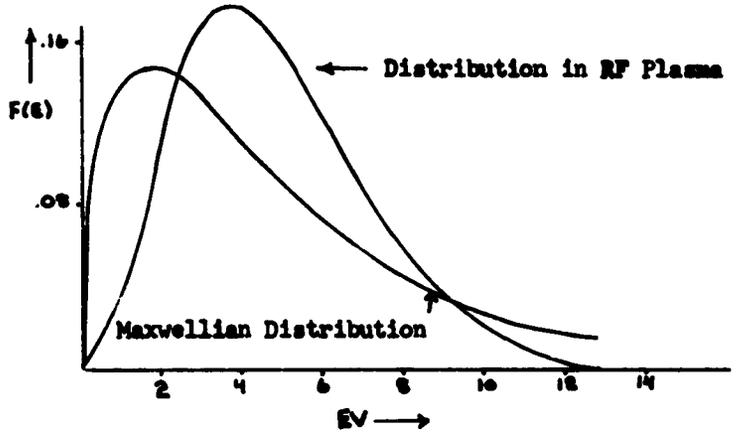

(b)

Probe at 5.1 cm from Reference Electrode

Fig. 21

Energy Distribution in RF Plasma

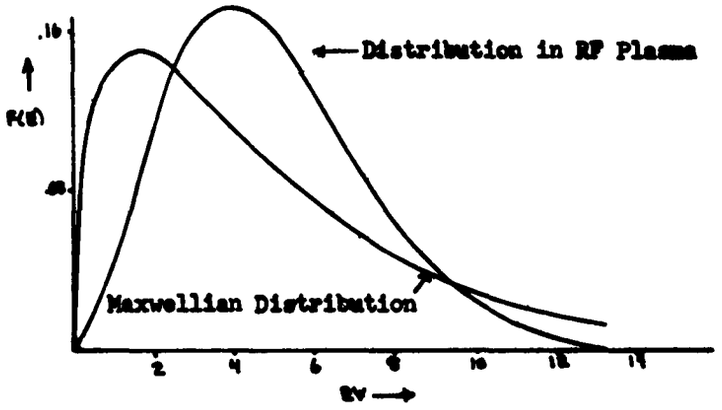

(a)

Probe at 6.3 cm from Reference Electrode

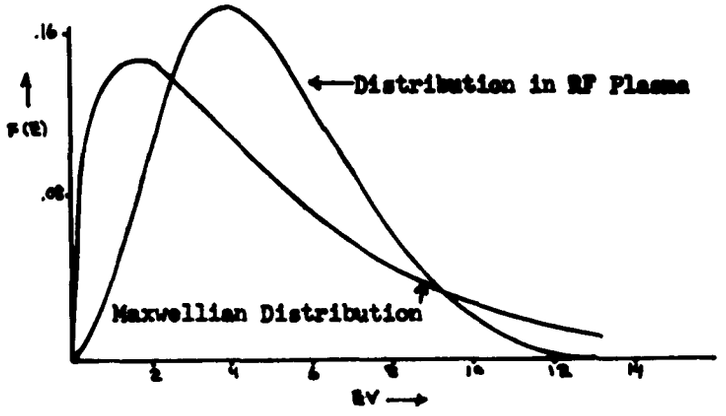

(b)

Probe at 8.9 cm from Reference Electrode

Fig. 22

Energy Distribution in RF Plasma

with those energies or higher can excite argon atoms and hence will lose some or all of their energy. The first ionization potential of argon occurs at 15.68 ev (Ref 5:2549). As the energy distribution curves in Fig. 11 indicate, no electrons collected by the probe at any of the points where probe measurements were made were energetic enough to cause ionization. At least they were not present in detectable quantities.

The fact that the discharge was self-sustaining may be explained by two possibilities. First, it has been mentioned that argon has two metastable states. Metastable states have the characteristic of being comparatively long-lived. Their decay time is on the order of milliseconds versus a decay time of 10^{-8} seconds for a non-metastable state (Ref 14:15). Thus it is possible for ionization in the tube to occur in steps, i.e., an argon atom may be excited by an electron and then subsequently ionized by another electron.

Another possibility is that ionization takes place at the outer extremities of the tube. This is quite logical because as mentioned previously the local value of the electron energy is fixed by the local value of E. Since the field intensity decreases with the radius as Fig. 19 indicates, the electron energies would be expected to have lower values at the center of the tube than at its outer extremities. Diffusion into the center of the tube by the fast electrons is hindered by the electric field. The electrons will have a tendency to follow the E field lines which are radial about the center of the tube. Electrons penetrating into the center would have

to be scattered inwardly and this inward scatter would be hindered by inelastic scattering. The field should have a significant effect on the motion of the electrons because, as will be seen, the ratio of collision frequency to field frequency was about 3 to 1.

Table I shows the variation of the average energy of the electrons and also the variation of plasma density for various points along the axis of the tube. Many additional measurements along the axis of the tube need to be made before an explanation of this variation is attempted.

Table I

Average Energy of Electrons and Plasma Density at Various Probe Positions Along Tube Axis

Position (cm)	Average Energy (ev)	Plasma Density (electrons/cm^3)
2.5	4.67	3.08×10^{10}
3.8	5.13	3.13×10^{10}
5.1	4.84	3.48×10^{10}
6.3	4.84	3.28×10^{10}
8.9	4.84	3.0×10^{10}

Effect of Magnetic Field

It is obvious that the RF electric field prevents the electrons from achieving a Maxwellian distribution by continually supplying energy to them. What effect, if any, a magnetic field has on the electrons was investigated by supplying an external DC magnetic field to the plasma.

From a classical physics standpoint, a magnetic field does not change the magnitude of the velocity of the charged particle but only its direction. Thus the kinetic energy of the particle should remain the same. Probe curves were taken with and without an external magnetic field present, and they indicated that the density of the plasma was increased by a factor of 1.6 with the magnetic field present. Second derivative curves were also taken, and the second derivative curve with the magnetic field present matched perfectly the curve without the magnetic field, indicating that this external magnetic field had no effect on the energy distribution of the electrons. Thus it is reasonable to assume that the alternating magnetic field present in the plasma does not affect the energy distribution of the electrons either.

Deriving a distribution function that would predict the energy distribution of the electrons in the tube is an exceedingly difficult task and was not undertaken by this author. It is complicated by the fact that the distribution function will be a function of the electric field intensity and this intensity varies with the radius of the tube. The problem is even further complicated by the fact that in this

investigation the collision frequency as will be seen in the following paragraph was comparable to the exciting frequency. Thus, the task of constructing a model which describes the events occurring in the tube is very difficult.

Calculation of Collision Frequency

The calculation of the electron collision frequency in the dense mode was done by first determining the electron mean free path for elastic collision by use of the following formula (Ref 2:3):

$$\lambda = \frac{1}{P_0 P_c} \tag{62}$$

where λ is mean free path,

P_c is a measure of collision probability, and

P_0 is the reduced pressure in mm Mercury, i.e., $P_0 = \frac{P273}{T}$.

Using 4.8 ev as the average energy of the electron $P_c = 32$ (Ref 2:7). With $T = 293^{\circ}K$ Eq (62) becomes

$$\lambda = \frac{293^{\circ}K}{.2 \times 273 \times 32} = 1.58 \text{ cm}$$

Collision frequency is related to λ by the following equation

$$\nu = \frac{V}{\lambda} \tag{63}$$

Using $\lambda = 1.58$ and 1.16×10^7 cm/second as the value of the average electron velocity which was calculated by the computer

$$\nu = \frac{1.16 \times 10^7}{1.58} = 73.4 \times 10^6 \text{ collisions/sec} \tag{64}$$

Calculation of Percent of Ionization

The percentage of ionization of the gas in the bright mode was also calculated by first finding the number of gas atoms/cm^3 in the tube before the generation of the plasma and then comparing this number to the plasma density which was calculated by the computer. Letting the volume of the gas in the tube be V_1 at 0.2 mm Mercury at 293°K, the volume of the gas at STP is given by

$$V_0 = \frac{.2 \times V_1 \times 273}{293 \times 760} = .000245V_1 \tag{65}$$

Since there are 6.025×10^{23} atoms/mole and a mole of argon occupies 22,400 cm^3, the number of argon atoms in the tube is

$$\frac{6.025 \times 10^{23}}{22,400} \times .000245V_1 = 6.59V_1 \times 10^{15} \text{ atoms} \tag{66}$$

$$\frac{6.59V_1 \times 10^{15}}{V_1} = 6.59 \times 10^{15} \text{ atoms/cm}^3 \tag{67}$$

The average of the plasma density in Table I is 3.31×10^{10}. Therefore for the dense mode along the tube axis

$$\% \text{ ionization} = \frac{3.31 \times 10^{10}}{6.59 \times 10^{15}} \times 100 = .00050\% \tag{68}$$

Sources of Errors

The principal sources of calculable errors in the experiment may be attributed to reading of the ordinates of the second derivative curves. The values of the average energy are only good to two significant figures. Different data from the same second derivative curve were fed into the computer on two different occasions and the difference in average energy was 0.03 ev. The same thing was tried on another curve giving a difference in average energy of 0.08 ev.

Another source of error is in the probe itself. The probe does disturb the plasma to a certain extent. Studies made in the Electronic Technology Laboratory indicate that the distortion is most apparent at potentials near plasma potential. This would introduce errors in the low end of the distribution spectrum. The amount of distortion introduced by the probe has not yet been fully investigated.

In deriving Eq (46) it was assumed that the current collected by the probe was purely an electron current. In actuality in the electron-retarding region the current is composed of both electrons and ions. The ion current is approximately linear in the ion saturation region as Fig. 17 indicates and may be linearly extrapolated to zero for less negative voltages (Ref 7:594). If it were completely linear in the extrapolated region, then the ion current would have no effect on the second derivative curve as the second derivative of a linear equation is everywhere zero. If it is not linear, the effect will still be small because the ion current must monotonically go to zero at a potential slightly more positive than plasma potential and in

examining Fig. 17 this does not permit the ion current to be very concave downward. Thus any errors introduced by the ion current in the second derivative curves and in the resultant energy distribution curves should be extremely small.

Conclusions and Recommendations

The objective of determining the feasibility of making probe energy distribution measurements in an RF plasma was accomplished and energy distribution measurements were made along the axis of the tube. The results indicated that the assumption (which is often made for convenience) that the distribution is Maxwellian is not a good one.

There are many additional experiments which should be performed on the tube in order to understand more fully the electron energy distribution of an RF plasma. Measurements should be made at different tube pressures to see what effect changing the E/p ratio has on the energy distribution. The exciting frequency should also be varied to see what effect it has on the plasma energy distribution, if any. This latter experiment requires a push-pull transmitter since variable frequency measurements with the experimental set-up used for this report are impractical.

An experiment should be devised to see how isotropic the electrons are along the axis of the tube. This could be accomplished by changing the orientation of a plane probe in the tube and examining the resulting probe curves. This experiment is important because spherical probe

theory is based on isotropic distribution of electrons. If the field is weak near the axis of the tube, the distribution may very well be quite isotropic, but this should be investigated.

If the tube is constructed with a small movable loop that can be extended from the tube wall to the center of the tube, then the magnetic field may be probed. If the magnetic field is zero in the interior of the plasma, then the associated electric field must be zero and the plasma is thus effectively acting as a shield to the electric field.

Finally, since this experiment is so dependent on symmetry it is recommended that in future experiments a reference electrode identical to the one used in this experiment be placed in the bottom of the tube to further symmetrize the conditions in the plasma.

Bibliography

1. "Amateur Scientist: Investigation of Electrical Discharge Without Expensive Vacuum Pumps." Scientific American, 194:132-136 (February 1956).

2. Brown, Sanborn C. Basic Data of Plasma Physics. New York: John Wiley and Sons, Inc., 1959.

3. Eckert, Hans U. "Diffusion Theory of Electrodeless Ring Discharge." Journal of Applied Physics, 33:2780-2788 (September 1962).

4. Fetz, H., and H. Oechsner. "Über die Untersuchung eines Hochfrequenzplasmas mit Hilfe einer Gleichstromsonde." Zeits für Angewandte Physik, 12:250-253 (June 1960).

5. Handbook of Chemistry and Physics (Forty-Second Edition). Cleveland: The Chemical Rubber Publishing Co., 1961.

6. Hellund, E. J. The Plasma State. New York: Reinhold Publishing Corp., 1961.

7. Langmuir, Irving. "Scattering of Electrons in Ionized Gases." Physical Review, 26:585-613 (November 1925).

8. Linhart, J. G. Plasma Physics. Amsterdam: North Holland Publishing Co., 1960.

9. Medicus, G., et al. "Automatic Plotting Device for the Second Derivative of Langmuir Probe Curves." The Review of Scientific Instruments, 34:231-237 (March 1963).

10. Medicus, G. "Simple Way to Obtain the Velocity Distribution of the Electrons in Gas Discharge Plasmas from Probe Curves." Journal of Applied Physics, 27:1242-1248 (October 1956).

11. ———. "Theory of Electron Collection of Spherical Probes." Journal of Applied Physics, 32:2512-2520 (December 1961).

12. Millman, J., and S. Seeley. Electronics. New York: McGraw-Hill Book Co. Inc., 1941.

13. Mott-Smith, H. M., and I. Langmuir. "The Theory of Collectors in Gaseous Discharges." Physical Review, 28:727-763 (October 1926).

14. Penning, F. M. Electrical Discharges In Gases. New York: The MacMillan Co., 1957.

15. The Radio Amateur's Handbook (Thirty-Ninth Edition). West Hartford, Connecticut: The American Radio League, Inc., 1962.

16. Von Engel, A. Ionized Gases. London: Oxford University Press, 1955.

Appendix A

Computer Program for Data Reduction*

The program used in reducing the data uses Eq (46) to obtain the unnormalised energy distribution ordinates. The integral $\int_{E_V}^{E_{max}} F(E)dE$ is evaluated and normalised to 1 by multiplying it by a normalizing factor. Simpson's Rule is used in performing the integration. Then each energy distribution ordinate calculated by Eq (46) is multiplied by the same normalizing factor mentioned above and thus the distribution curves plotted on pages 57, 59, and 60 are normalised.

This program uses the AFIT Fortran System. The AFIT Processer, Loader and Subroutine decks may be obtained from the IBM Library. For input data an even number of equal increments must be taken along the horizontal axis of the second derivative curves since as mentioned above Simpson's Rule is used in the normalisation of the energy distribution ordinates. The data must be read into the computer in the following order: H, N, CPP, E(I)'s, and SD(I)'s. These variables are defined in the Dictionary of Variables shown on the following page.

*Program for the IBM 1620 Digital Computer.

```
      DIMENSIØN E(200),SD(200),GE(200)
      READ,H,N,CPP
      BK=.8617E-04
      PI=3.14159
      RP=.00027
      EM=.91083E-30
      Q=.16021E-18
      DØ 1 I=1,N
1     READ,E(I)
      DØ 2 I=1,N
2     READ,SD(I )
      DØ 3 I=1,N
3     GE(I)=SD(I)*SQRT(E(I))
      MM=1
      NN=N-1
4     A=0.
      B=0.
      J=0
5     J=J+1
      L=2*J
      M=2*J+1
      B=B+GE(L)
      IF(NN-L)7,7,6
6     A=A+GE(M)
      GØ TØ 5
```

```
7     GØ TØ (8,11),MM
8     AREE=(H*(GE(1)+GE(N)+4.*B+2.*A))/3.
      FØNE=1./AREE
      L=0
      PRINT 61
      PRINT 70
      DØ 10 I=1,N
      GE(I)=GE(I)*FØNE
      PRINT 62,I,GE(I)
      L=L+1
      IF(L-3)10,9,10
9     L=0
      PRINT 60
10    CØNTINUE
      GØ TØ 12
11    AVEN=(H*(GE(1)+GE(N)+4.*B+2.*A))/3.
      GØ TØ 14
12    DØ 13 I=1,N
13    GE(I)=GE(I)*E(I)
      MM=2
      GØ TØ 4
14    T=(AVEN*2.)/(3.*BK)
      L=0
      PRINT 63
      PRINT 70
```

```
      DØ 16 I=1,N
      BB=2./(SQRT(PI)*((BK*T)**1.5))
      SD(I)=BB*SQRT(E(I))*EXP(-(E(I)/(BK*T)))
      PRINT 64,I,SD(I)
      L=L+1
      IF(L-3)16,15,16
 5    L=0
      PRINT 60
16    CØNTINUE
      DØ 17 I=1,N
      SD(I)=SQRT(2.*E(I)*Q/EM)
17    GE(I)=GE(I)/E(I)
      JJ=1
18    A=0.
      B=0.
      LL=N-1
      DØ 19 I=1,LL
      B=.5*(SD(I+1)-SD(I))*(GE(I+1)+GE(I))
19    A=A+B
      GØ TØ (20,21),JJ
20    AREV=A
      GØ TØ 22
21    AREVW=A
      AVEV=AREVW/AREV
      GØ TØ 24
```

```
22    DØ 23 I=1,N
23    GE(I)=GE(I)*SD(I)
      JJ=2
      GØ TØ 18
      PD=(CPP)/(PI*(RP**2.)*Q*AVEV)
      PRINT 65,AVEN
      PRINT 66,AVEV
      PRINT 67,T
      PRINT 68,PD
60    FØRMAT(/7X)
61    FØRMAT(/30X,25HRF DISTRIBUTIØN ØRDINATES)
62    FØRMAT(2HGE14,1H=F6.4,7X)
63    FØRMAT(/30X,33HMAXWELLIAN DISTRIBUTIØN ØRDINATES)
64    FØRMAT(3HGEM14,1H=F6.4,6X)
65    FØRMAT(///20X,24HAVERAGE ELECTRØN ENERGY=F6.3,1X,2HEV)
66    FØRMAT(///20X,26HAVERAGE ELECTRØN VELØCITY=F9.0,1X,3HMPS)
67    FØRMAT(///20X,21HELECTRØN TEMPERATURE=F10.1,1X,9HDEGREES K)
68    FØRMAT(///20X,15HPLASMA DENSITY=E14.8,1X,17HELECTRØNS PER MTR)
70    FØRMAT(///7X)
      STØP
      END
```

Appendix B

Semi-log Plots of Second Derivative Curves

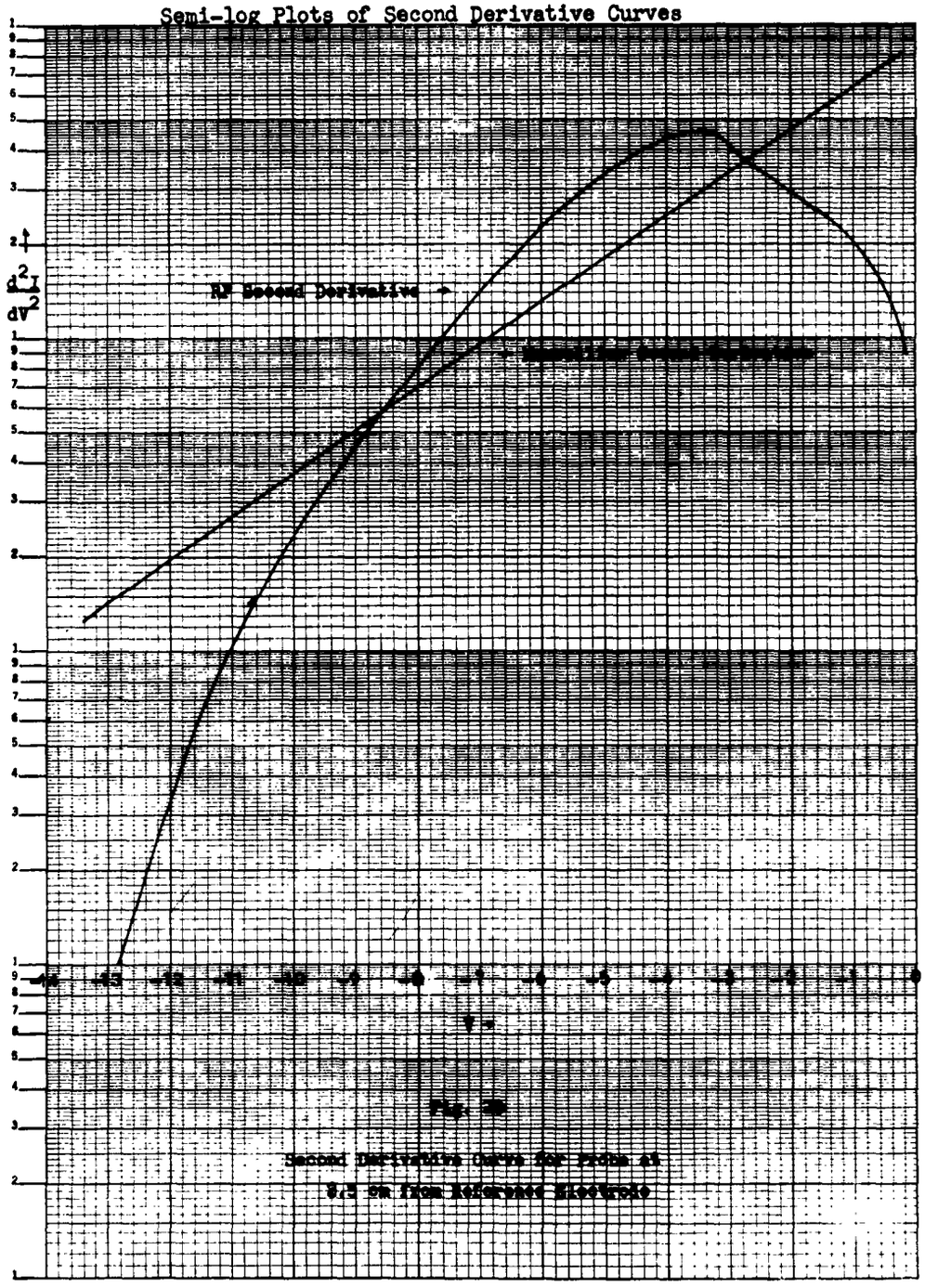

Fig. 2B

Second Derivative Curve for Probe at 0.5 cm from Reference Electrode

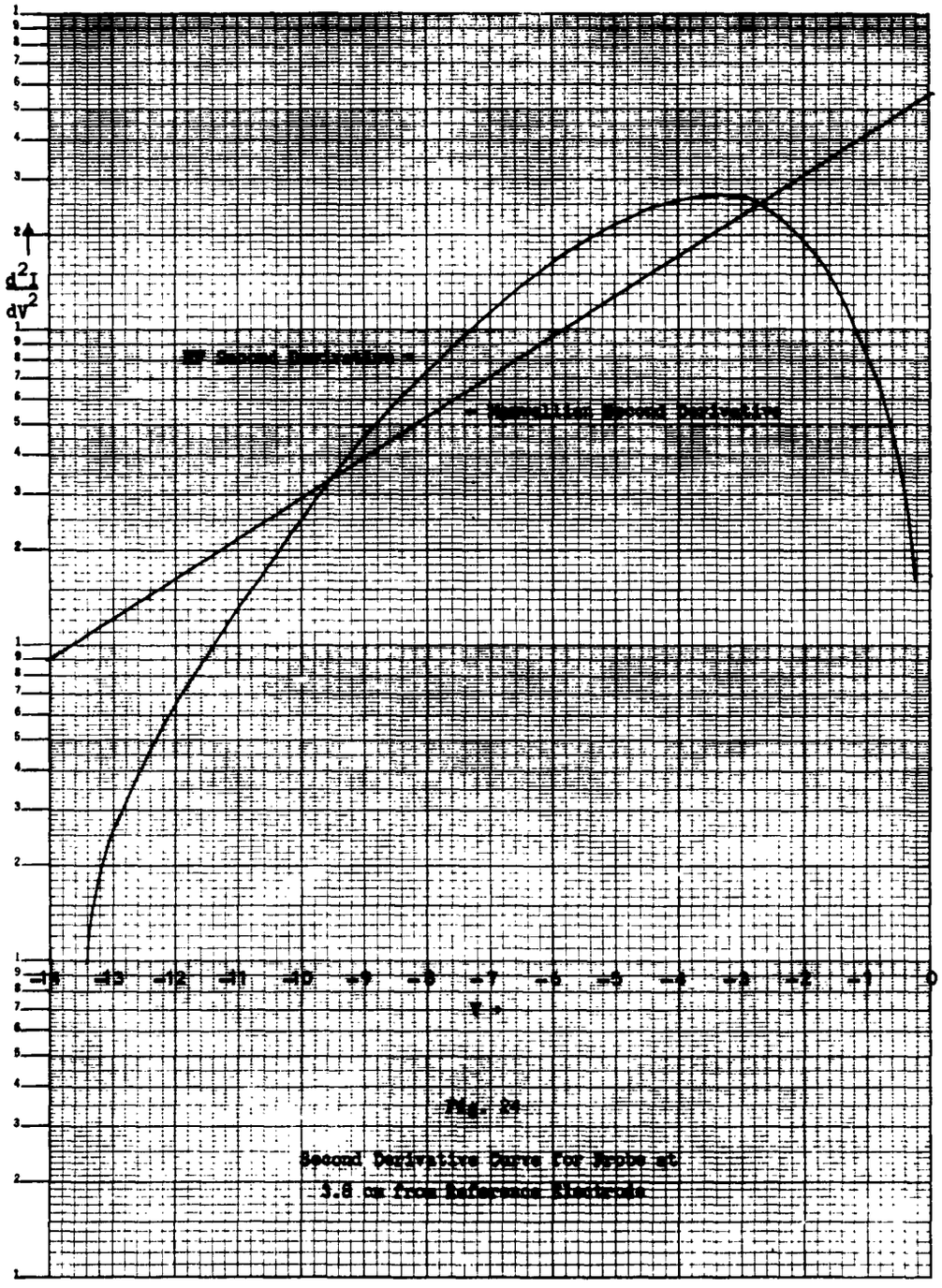

Fig. 24

Second Derivative Curve for Probe at 5.8 cm from Reference Electrode

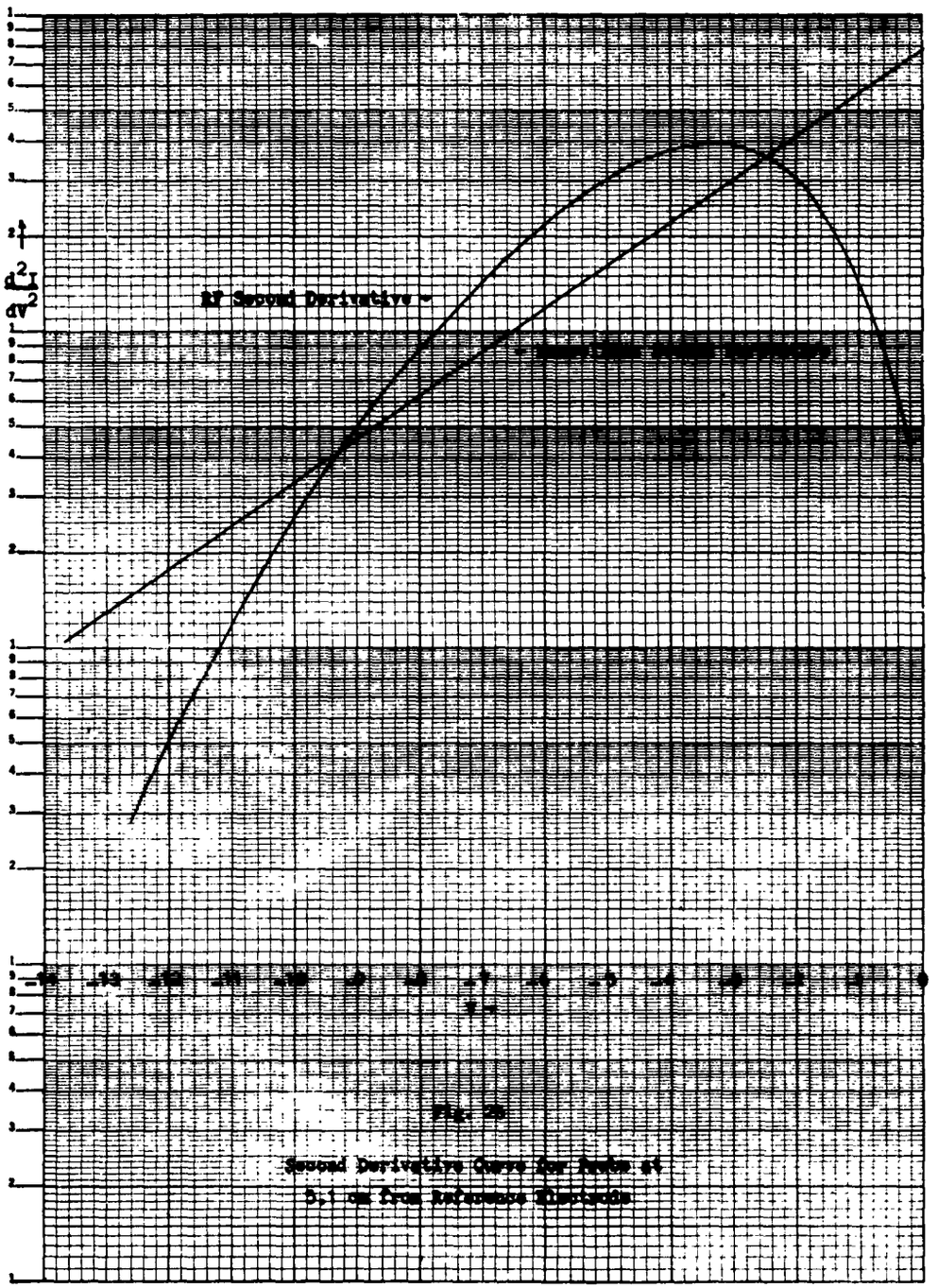

Fig. 2b

Second Derivative Curve for Probe at
5.1 cm from Reference Electrode

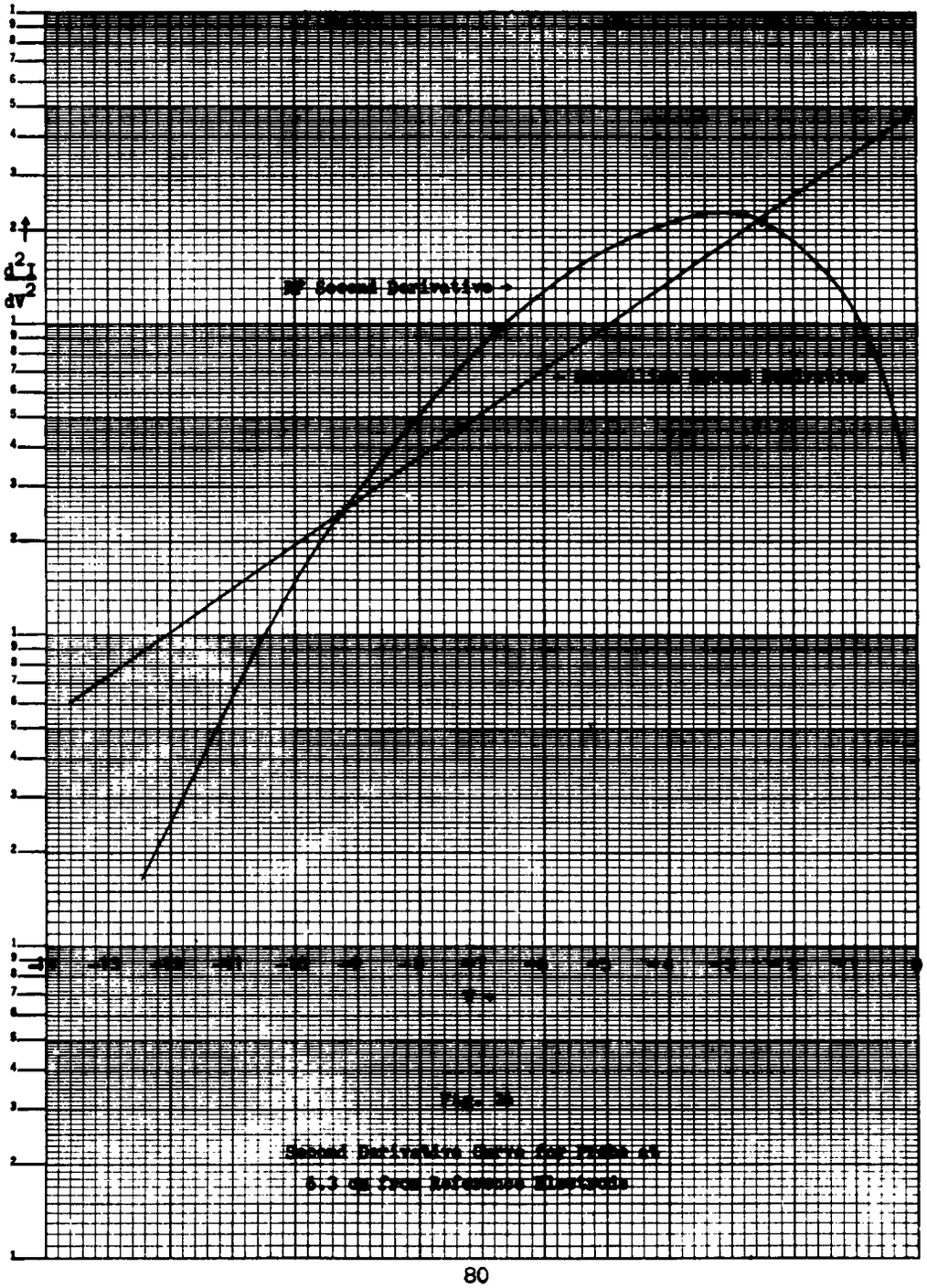
$\frac{d^2I}{dV^2}$
SP Second Derivative →
Fig. 36
Second Derivative Curve for Probe at
5.3 cm from Reference Electrode

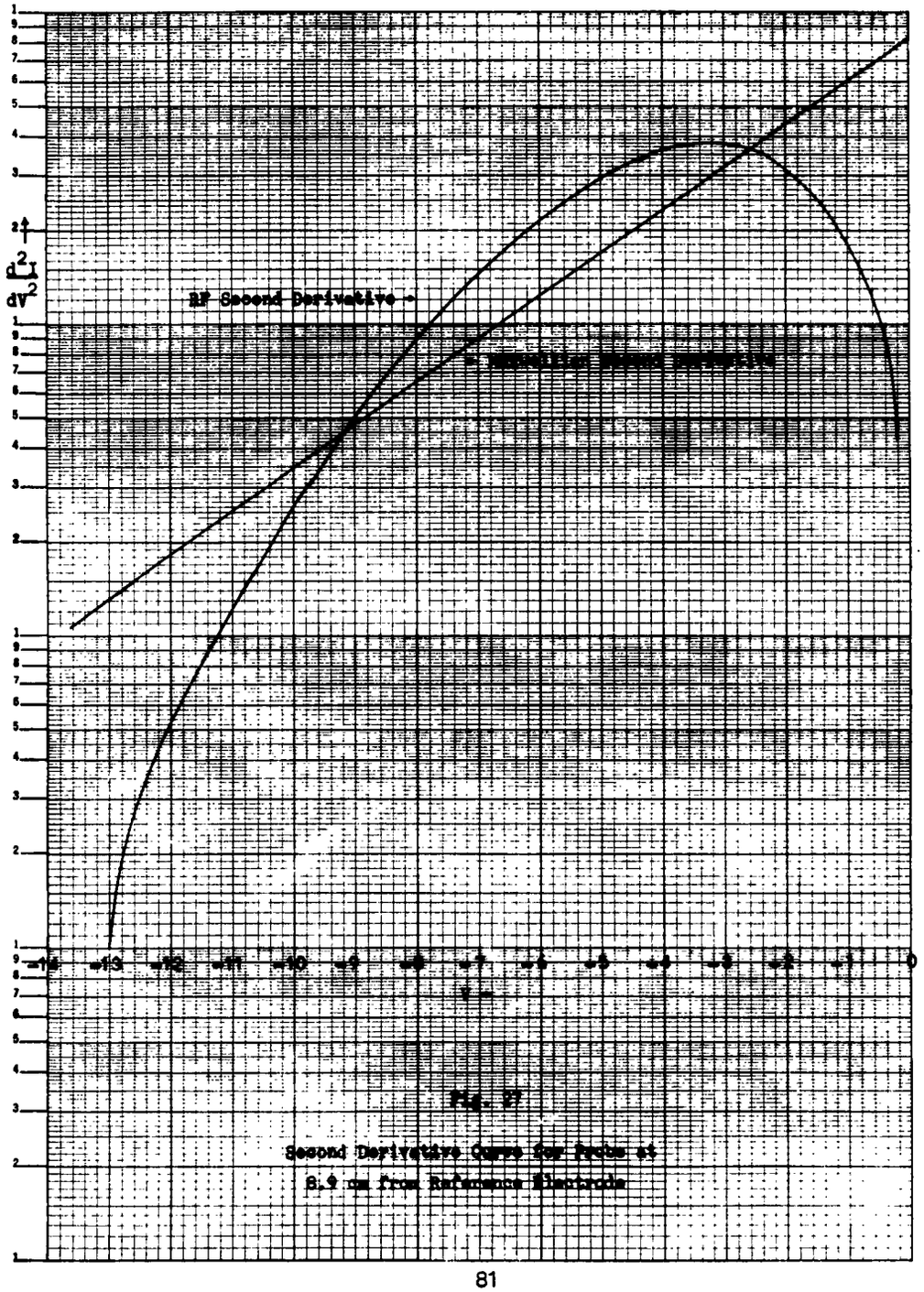

Fig. 27

Second Derivative Curve for Probe at
8.9 cm from Reference Electrode